CHAPTER 3

EFFECT OF ADSORPTION OF VAPOURS ON THE ELECTRICAL CONDUCTIVITY OF SOME POLYENE SEMICONDUCTORS : ADSORPTION AND DESORPTION KINETICS

3.1 Introduction

Adsorption of gases changes the semiconductive properties of both organic[1-6] and inorganic[7-10] solids. Adsorption of oxygen produces a pronounced increase of semiconduction current in phthalocyanine[1], anthracene[2,11,12] and chlorophylls[13]. Number of other gases also affect the current. Adsorption of various gases and vapours enhances the specific conductivity of β-carotene[4,6]. It has been observed that the conductivity change is generally reversible[5,6,14] — one can return to the initial value of conductivity simply by desorbing the gases or vapours.

Gray and Darby[10] have studied in detail the semi-conductivity changes during the adsorption and desorption of oxygen gas on oxides of copper, nickel, manganese and zinc of extremely high purity. They have considered the first order, second-order and exponential relationships $(dm/dt) = Km$, $(dm/dt) = Km^2$ and $(dm/dt) = K \exp(-\epsilon m)$ respectively where m is the number of adsorbed atoms at time t; K and ϵ are constants. These relationships have been derived by many authors making direct measurements of the amount of gases adsorbed Gray et al[10] have shown that the exponential plot is a better over-all approximation for the complex order process than for one obeying the first order kinetics, or a combination of the second and first order processes at the initial and final period of adsorption respectively. In working out the kinetics, Gray and Darby have assumed that the measured conductivity is either proportional to $\sqrt{m}$ or to m.

In case of hydration of proteins[15] and adsorption of gases on β -carotene[6], it has been observed that the adsorption-time curves follow the Roginsky-Zeldovichs'[16,17] exponential equation in a slightly modified form. The derivation of this equation assumes that the rate of adsorption (dm/dt) possesses an activation energy which increases linearly with the amount (m) of the adsorbed gas or vapour,

$$\frac{dm}{dt} = A \exp(-\beta m / kT) \qquad (3.1)$$

where for a particular pressure A and β are constants. These workers, unlike that of Gray et al.[10] have shown with a good degree of certainty that at a constant temperature and for lower percentage of gas or vapour adsorption, the relationship between the conductivity (σ) and the amount of gas or vapour adsorbed is given by[5,6,18]

$$\sigma_A(m) = \sigma_V \exp(\alpha m) \qquad (3.2)$$

where σ_V and σ_A are the specific conductivities before and after adsorption of m percent of gas or vapour; α is a constant.

However, experiments clearly show that there is a direct correlation between the rate of adsorption of gases or vapours and the change in semiconduction current. It is therefore, necessary to examine this correlation in detail to determine the most reasonable and accurate correlation. As the rate of adsorption of gases or vapours depends on its pressure, the consideration of formal adsorption kinetics is incomplete without an examination of the pressure

dependence of the adsorption process and hence of the conductivity change.

In this chapter, we first discuss how the conductivity of polyene semiconductors depends on the pressure of the adsorbed vapours and then examine the validity of the Hopinsky - Zeldovich relation.

3.2 Experimental and Results

3.2.1 Semiconduction of some polyenes and the effect of adsorption of vapours on the semiconduction current.

The effects of adsorption of some vapours were studied in the usual manner as described in the previous chapter. The sandwich cell was temperature cycled and in addition to that dry nitrogen gas was allowed to pass through the chamber to desorb any vapour or gas adsorbed by the sample prior to the experiment. The cell was then kept at room temperature (28°C) and the carrier gas, dry nitrogen, was passed through the reagent liquid which was kept at a constant temperature to maintain a required vapour pressure. After a few moments as the powder sample started to adsorb the vapour from the chamber-atmosphere, the current began to increase and attained a saturation value after half an hour approximately. The current enhancement was by several orders of magnitude in some cases. The result of such a measurement for ethyl acetate vapour adsorption in vitamin A alcohol is shown in Fig. 3.1. The curve (b) of Fig. 3.1

FIG. 3.1 : The change in dark current in a vitamin A alcohol powder cell kept at 25°C with (a) adsorption and (b) desorption of ethyl acetate vapour at 43.5 mm pressure.

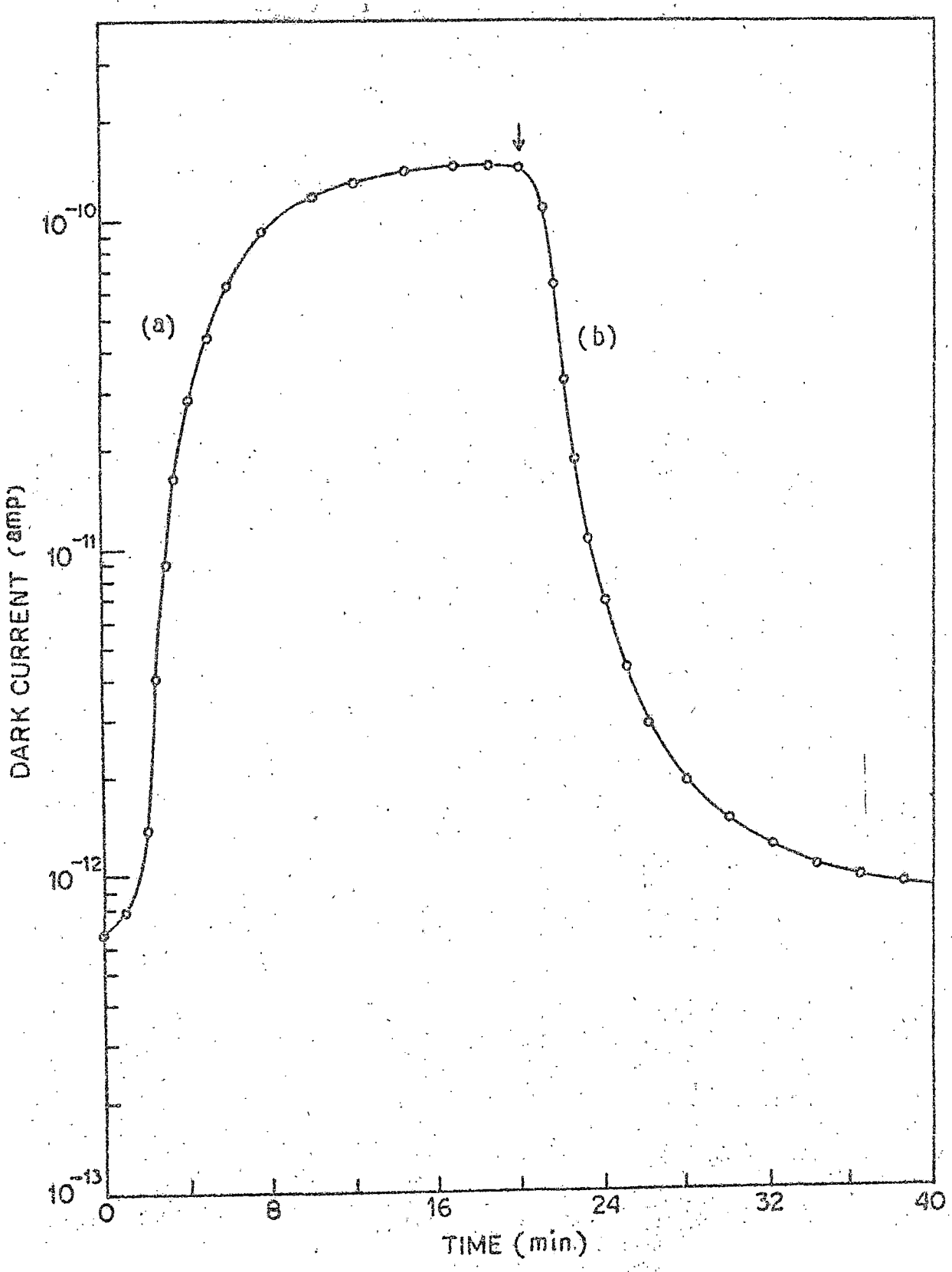

FIG: 3.1

shows the decrease in conductivity back to its initial value when the chamber is flushed with dry nitrogen gas and the vapour is desorbed from the crystallite surfaces. The arrow indicates the time when desorption starts. Such adsorption and desorption kinetic curves for vitamin A acetate, β -apo-8'-carotenal, astacene and methyl bixin for ethyl acetate vapour adsorption are shown in Figs. 3.2 - 3.5, respectively. All these curves show excellent reversibility of current on desorption of vapours. Similar curves are obtained for toluene, benzene, n-heptane, ethanol and methanol vapour adsorption also. The maximal value of current reached under particular experimental conditions, depends on the vapour pressure of the reagent liquid at its temperature and also on the temperature of the sample cell; time to reach this value depends also on the flow rate. To test the sensitivity of a particular polyene semiconductor for different vapours, saturation current values were noted after adsorption of various vapours at a fixed partial vapour pressure with a constant flow rate and a constant sample cell-temperature. The sensitivity as measured by σ_A/σ_V values of the different polyene semiconductors in sandwich cells for adsorption of various vapours are summarized in tables 3.1 and 3.2. Apparently, the sensitivity depends on the chemical nature of the adsorbed molecules.

3.3.2 Semiconduction as a function of vapour pressure

We have studied the magnitude of the current increase at a constant sample cell temperature as a function of the partial pressure of the vapours in the chamber. The temperature of the reagent liquid through which dry nitrogen gas was passed and fed

FIG. 8.2 : The change in dark current in a vitamin A acetate powder cell kept at 25°C with (a) adsorption and (b) desorption of ethyl acetate vapour at 42.0 mm pressure.

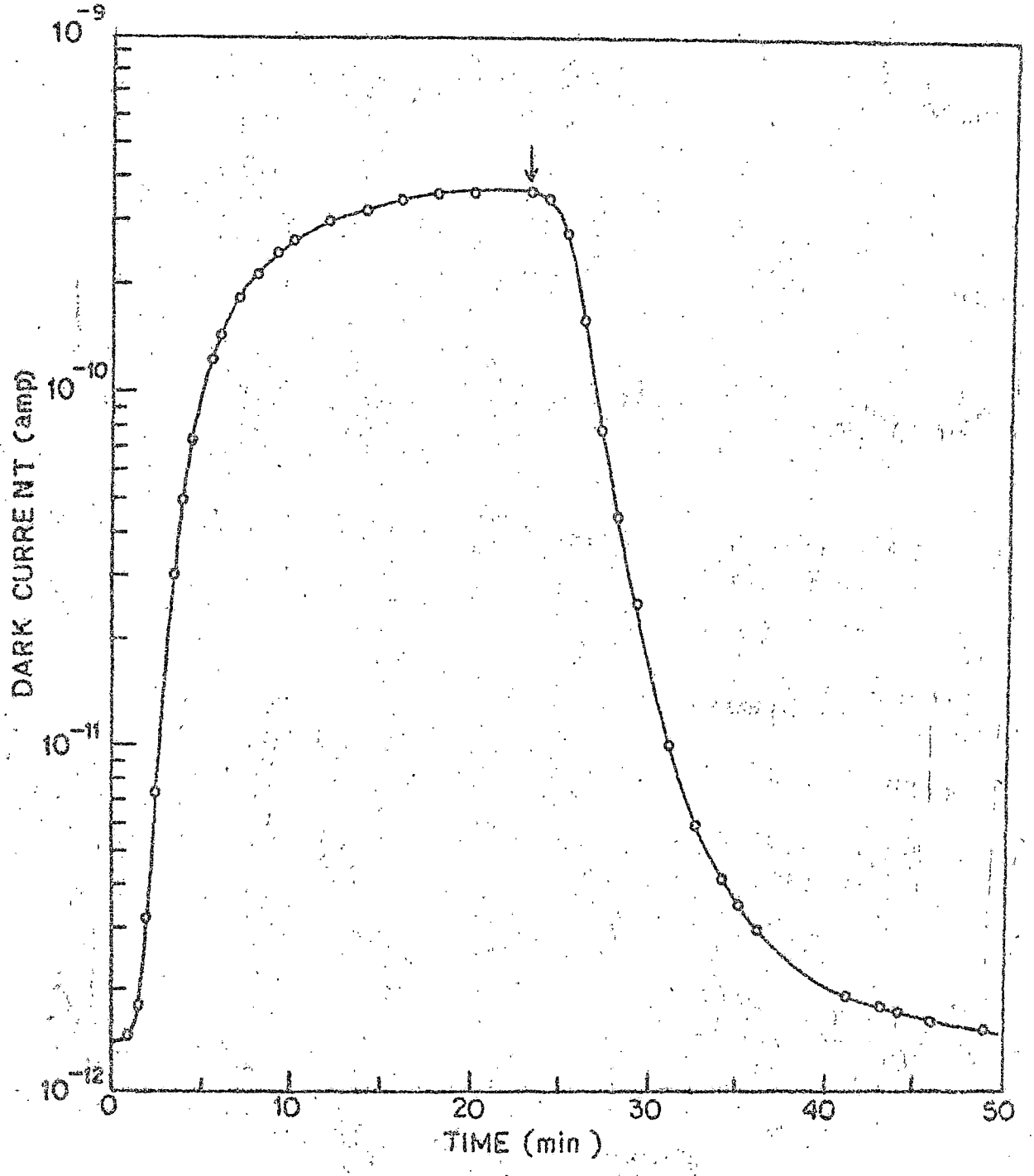

FIG. 3·2

FIG. 3.3 : The change in dark current in a β -apo-8'-carotenal powder cell kept at 25°C with (a) adsorption and (b) desorption of ethyl acetate vapour at 53.8 mm pressure.

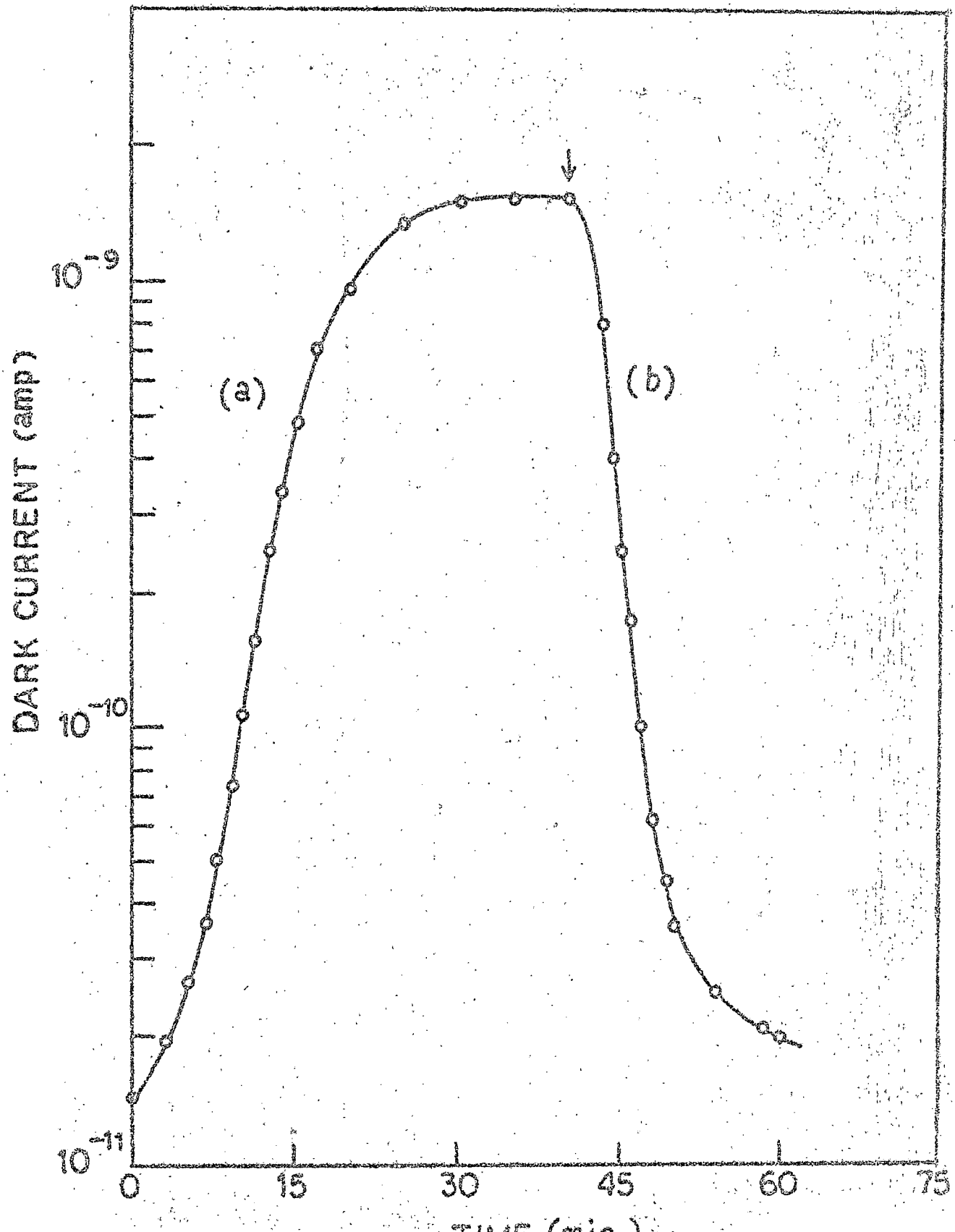

FIG. 3.3

FIG. 3.4 : The change in dark current in an anthracene powder cell kept at 25°C with (a) adsorption and (b) desorption of ethyl acetate vapour at 70.0 cm pressure.

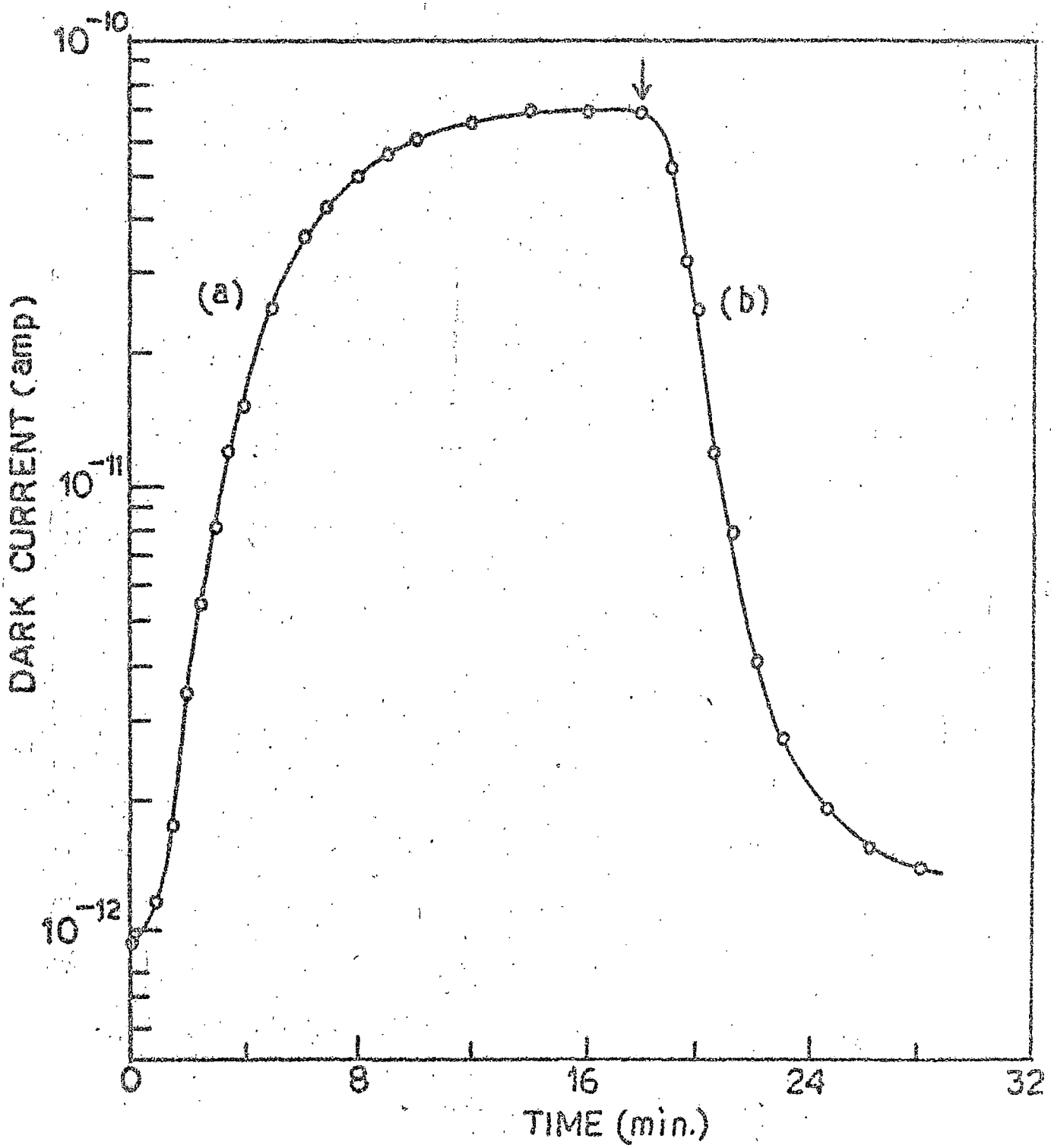

FIG. 3·4

FIG. 3.5 : The change in dark current in a methyl bixin powder cell kept at 25°C with (a) adsorption and (b) desorption of ethyl acetate vapour at 80.0 mm pressure.

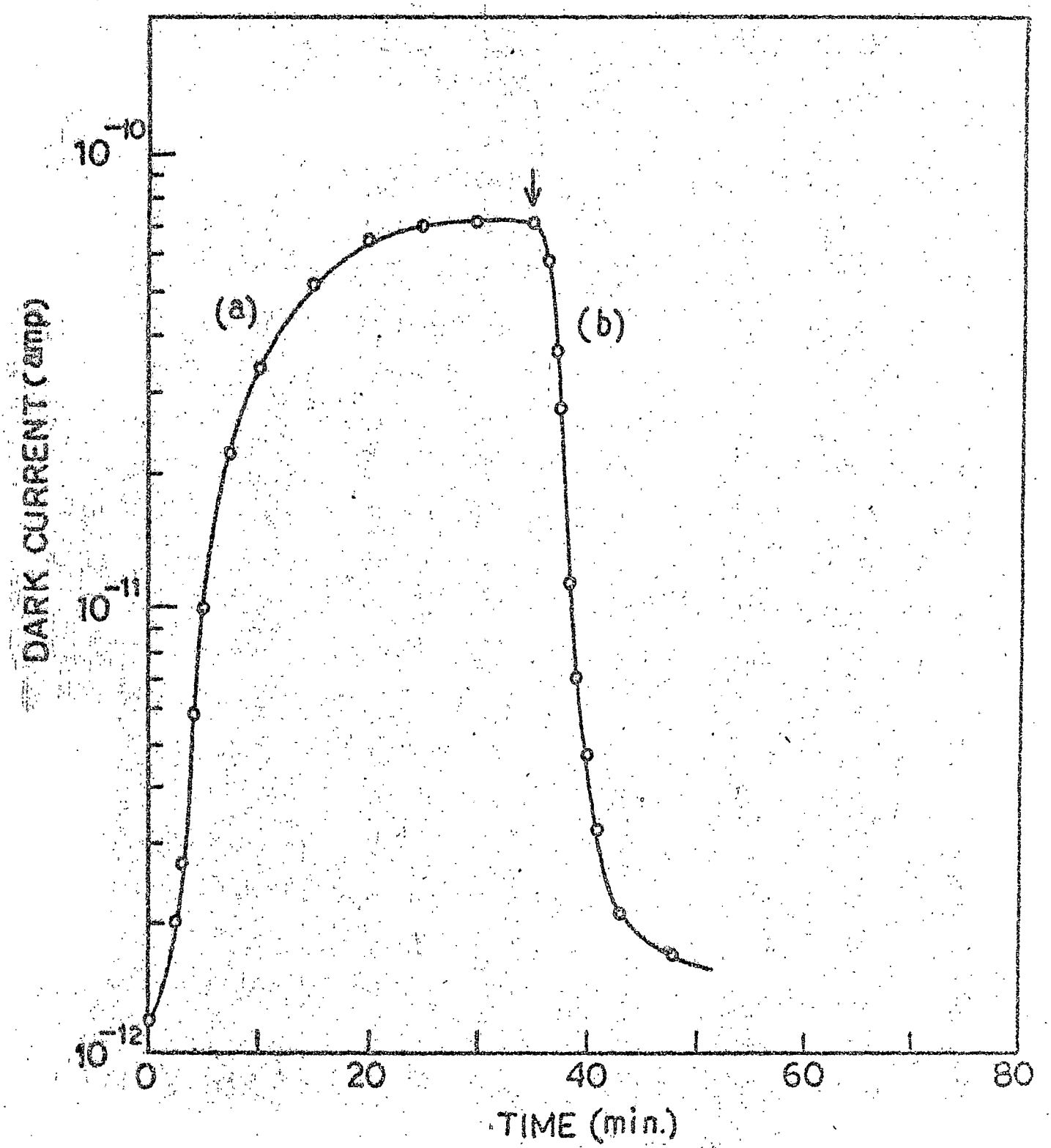

FIG. 3·5

Table - 3.1

Rise in the dark current in vitamin A (alcohol and acetate) powder cells at 12.5°C due to adsorption of various vapours at the same pressure of 40 mm.

Vapour adsorbed	Dielectric constant[1] at 25°C	Ionisation potential[2] (eV)	σ_A / σ_V	
			vitamin A alcohol	vitamin A acetate
Toluene	2.38	8.81	2.3×10^4	5.0×10^4
Benzene	2.28 (20°C)	9.24	6.7×10^3	1.7×10^4
Ethyl acetate	6.00	10.11	6.5×10^3	1.3×10^4
n-Heptane	1.93 (20°C)	10.35	4.0×10^3	3.8×10^3
Ethanol	24.30	10.50	3.0×10^2	2.0×10^3
Methanol	32.60	10.85	4.5×10	3.2×10^2

1. Ref. 19
2. Ref. 20 and 21

Table - 3.2

Rise in the dark current in the powder cells of some polyenes at 18.5°C due to adsorption of various vapours at the same pressure (p) for a particular polyene

Vapour adsorbed	Dielectric constant	Ionisation potential (eV)	σ_A / σ_V		
			β-apo-8'-carotenal p = 42 mm	Octacene p = 60 mm	Methyl bixin p = 60 mm
Toluene	2.38	8.81	7.3	1.8	1.6
Benzene	2.28 (20°C)	9.24	4.2	2.5	3.3
Ethyl acetate	6.00	10.11	5.0×10^2	1.5×10^2	1.0×10^1
n-Heptane	1.93 (20°C)	10.35	4.4	-	-
Ethanol	24.30	10.50	5.0×10^3	4.0×10^3	1.0×10^2
Methanol	32.60	10.85	6.5×10^2	5.0×10^2	3.3×10^1

into the conductivity chamber was varied. At a constant flow rate, the partial pressure of the reagent liquid vapour in the chamber atmosphere was proportional to the vapour pressure of the liquid at the temperature it was kept. The steady state current (i.e., saturation current) was noted for different vapour pressures. The kinetics for the dark current enhancement for different partial pressures of ethyl acetate ambient vapour for vitamin A alcohol, vitamin A acetate, β -apo-8'-carotenal, astacene and methyl bixin semiconductors are shown in Figs. 3.6 - 3.10 respectively.

3.3 Discussion

3.3.1 Sensitivity of the semiconductors for various vapours

It is seen from the tables 3.1 and 3.2 that there may be a rough correlation of the sensitivity of a semiconductor with the ionization potential of the adsorbed molecules but none with their static dielectric constant. As regards the correlation of conductivity enhancement with the ionization potential, the polyenes can be divided into two groups. In one, namely vitamin A alcohol and acetate the sensitivity is more, the lower is the ionization potential (table 3.1) while in the other, namely β -apo-8'-carotenal, astacene and methyl bixin, the sensitivity is more the higher is the ionization potential (table 3.2). Indeed, charge-transfer type of interaction has often been thought[22-24] to be responsible for the conductivity enhancement on gas or vapour adsorption.

FIG. 8.6 : The change in dark current in a vitamin A alcohol powder cell kept at 26°C after adsorption of ethyl acetate vapour at different pressures.

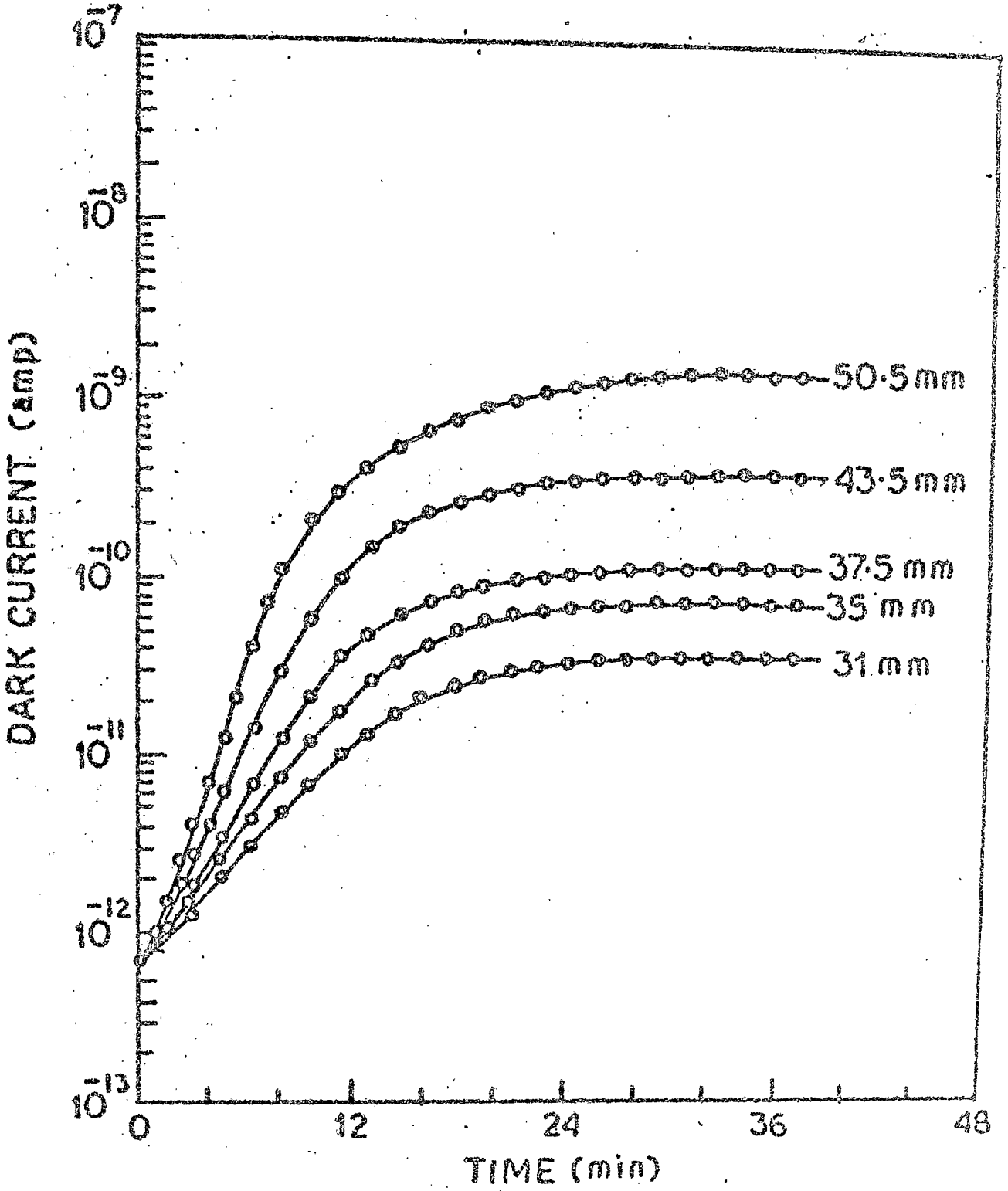
DARK CURRENT (amp)
10^{-7}
10^{-8}
10^{-9}
10^{-10}
10^{-11}
10^{-12}
10^{-13}
50·5 mm
43·5 mm
37·5 mm
35 mm
31 mm
0
12
24
36
48
TIME (min)

FIG. 3·6

FIG. 3.7 : The change in dark current in a vitamin A acetate powder cell kept at 25°C after adsorption of ethyl acetate vapour at different pressures.

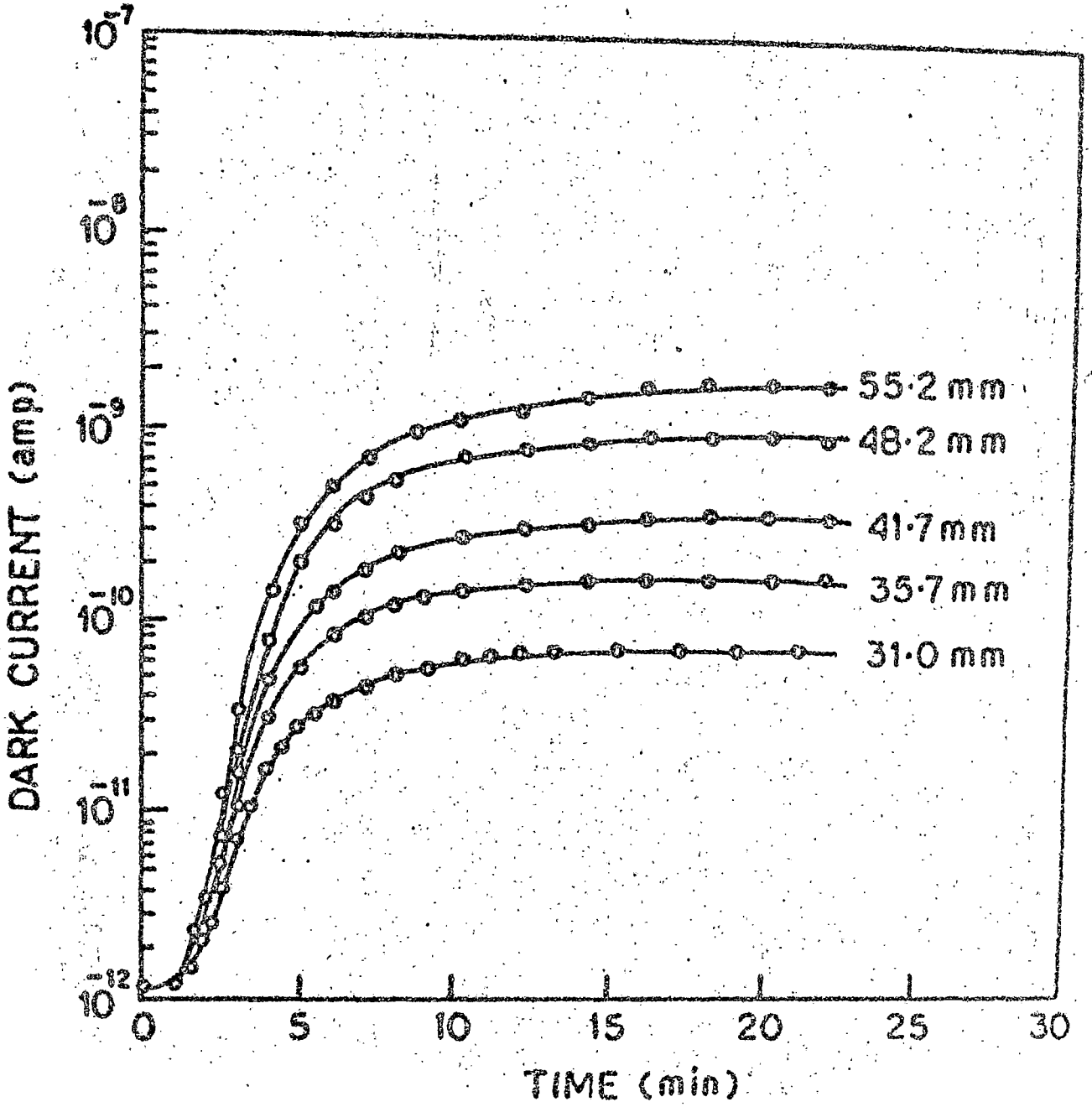
DARK CURRENT (amp)
10^{-7}
10^{-8}
10^{-9}
10^{-10}
10^{-11}
10^{-12}
55·2 mm
48·2 mm
41·7 mm
35·7 mm
31·0 mm
0
5
10
15
20
25
30
TIME (min)

FIG. 3·7

FIG. 3.8 : The change in dark current in a β -apo-8'-carotenal powder cell kept at 26°C after adsorption of ethyl acetate vapour at different pressures.

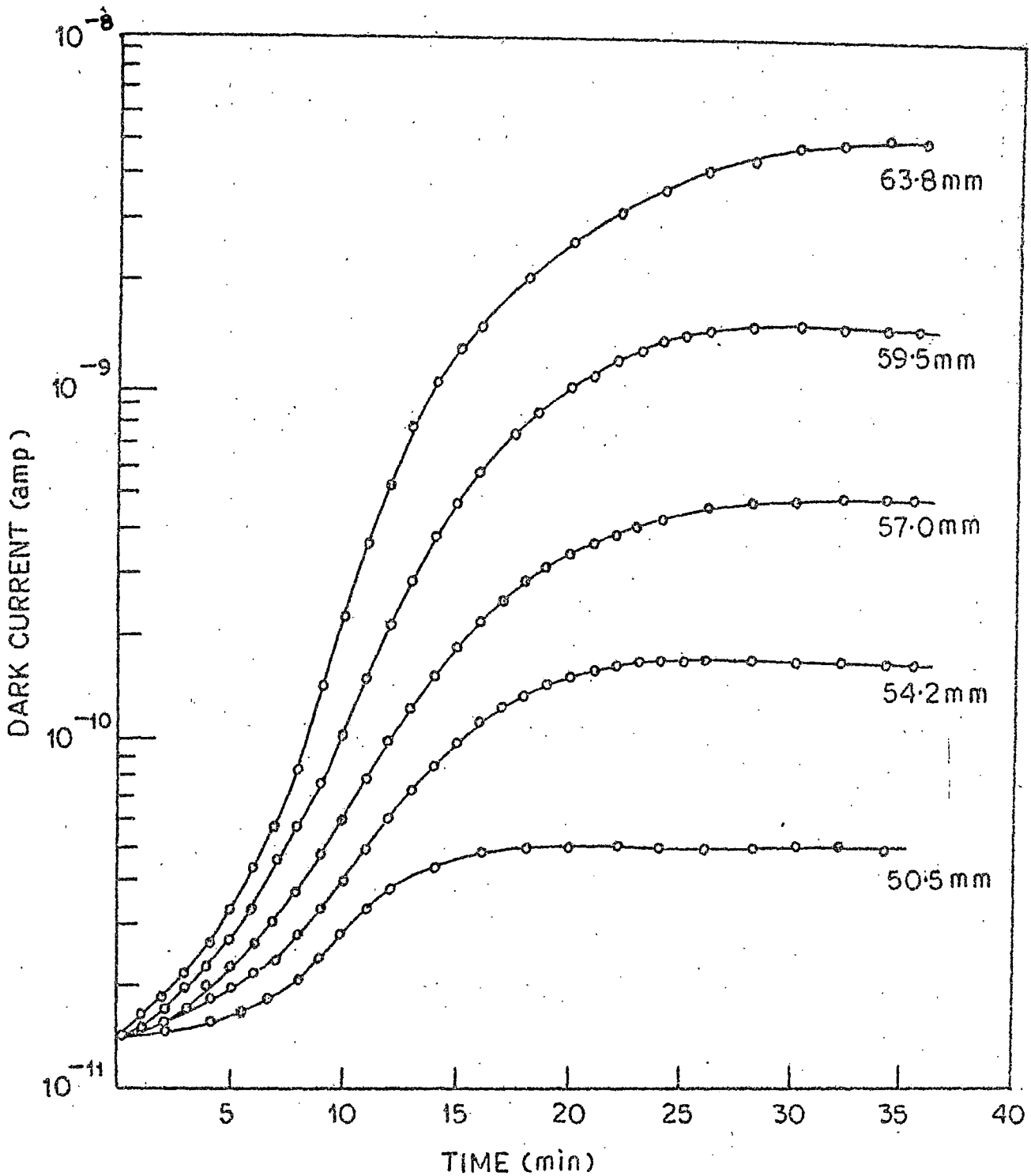
10^{-8}
10^{-9}
10^{-10}
10^{-11}
DARK CURRENT (amp)
63·8mm
59·5mm
57·0mm
54·2mm
50·5mm
5
10
15
20
25
30
35
40
TIME (min)

FIG. 3·8

FIG. 3.9 : The change in dark current in an antacene powder cell kept at 25°C after adsorption of ethyl acetate vapour at different pressures.

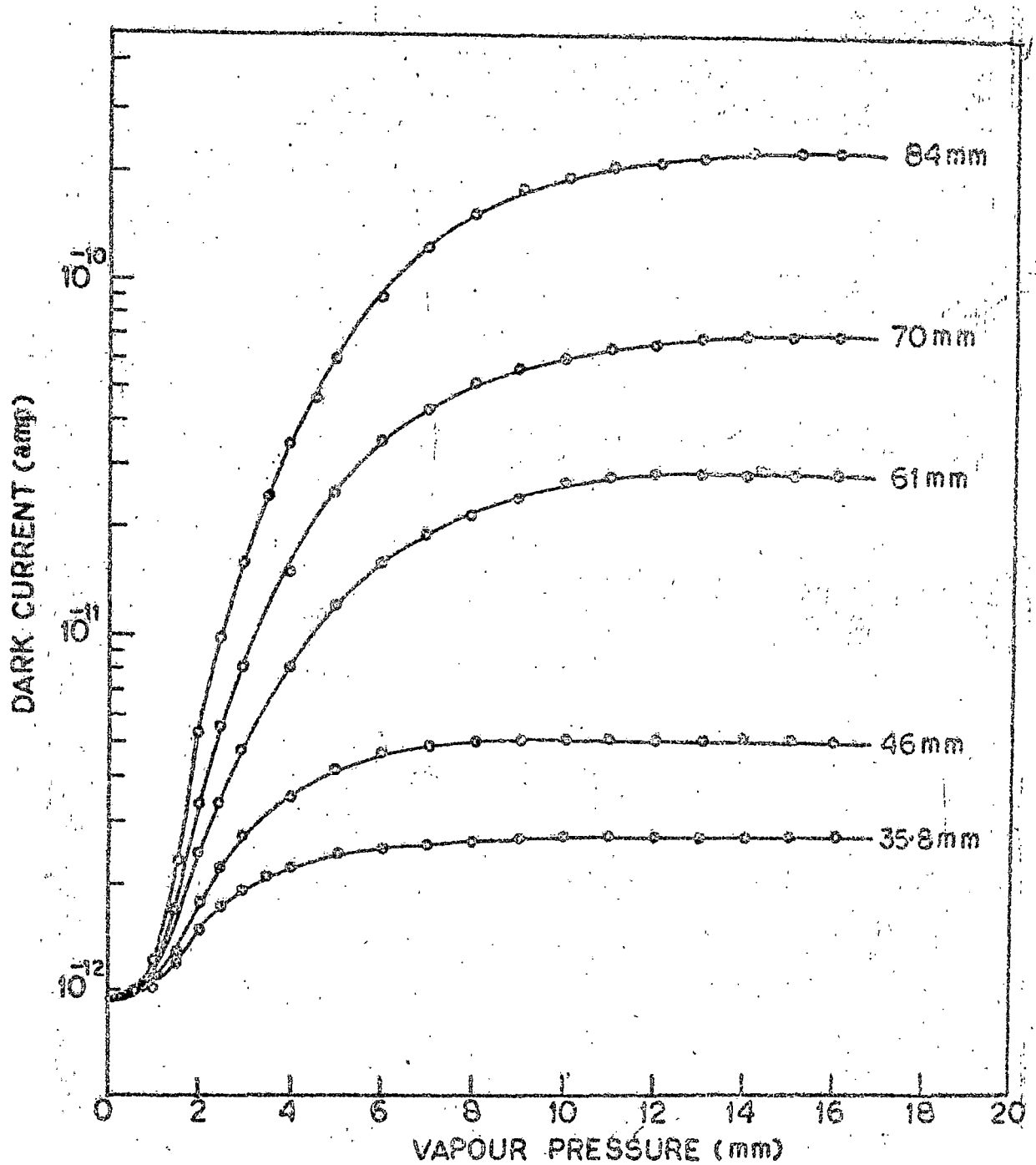
84 mm
70 mm
61 mm
46 mm
35·8 mm
10^{-10}
10^{-11}
10^{-12}
DARK CURRENT (amp)
0
2
4
6
8
10
12
14
16
18
20
VAPOUR PRESSURE (mm)

FIG. 3·9

FIG. 3.10 : The change in dark current in a methyl bixin powder cell kept at 25°C after adsorption of ethyl acetate vapour at different pressures.

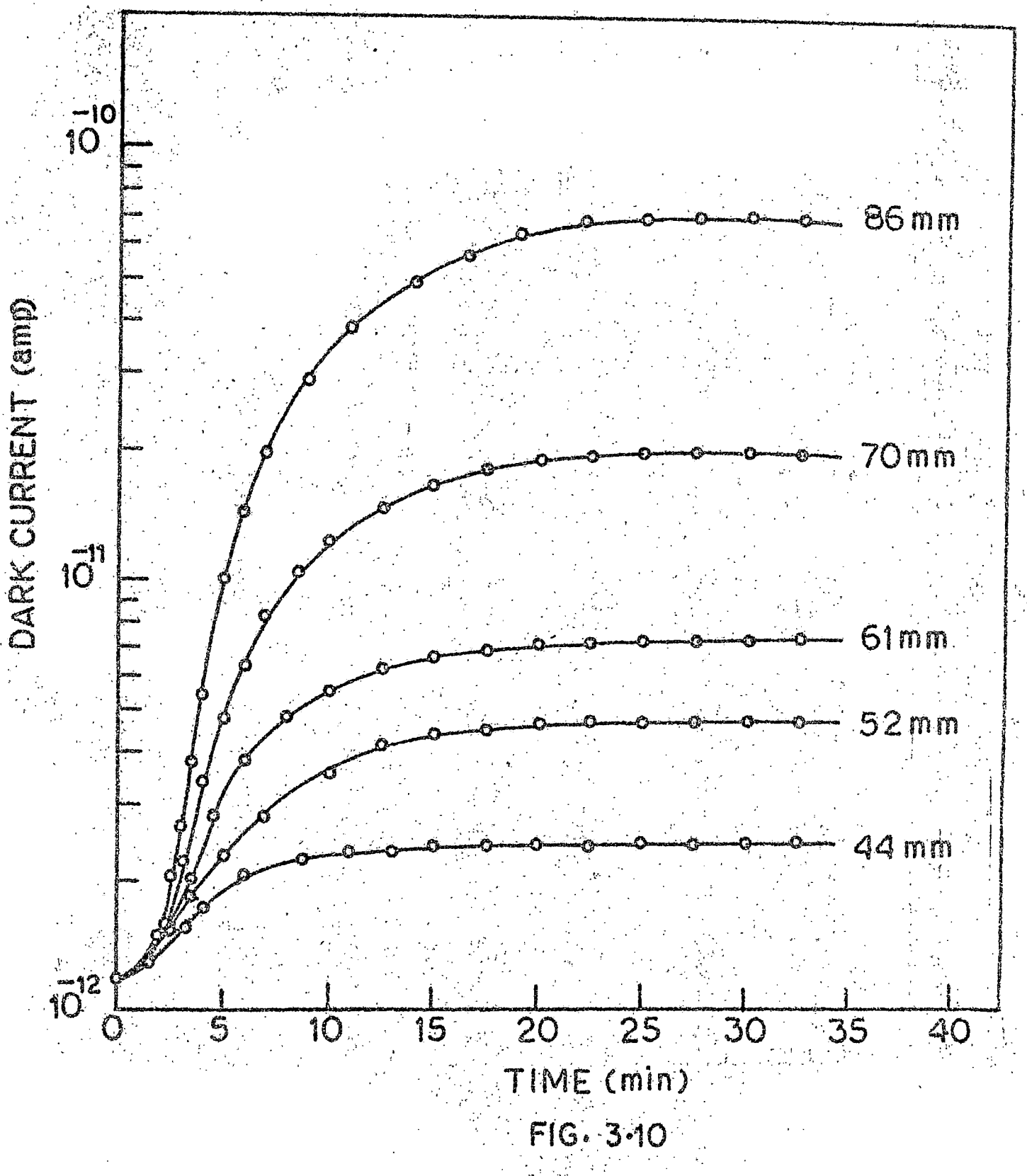
DARK CURRENT (amp)
10^{-10}
10^{-11}
10^{-12}
86 mm
70 mm
61 mm
52 mm
44 mm
0
5
10
15
20
25
30
35
40
TIME (min)

FIG. 3·10

3.3.2 Dependence of the conductivity on vapour pressure

The rise in conductivity of the polyene semiconductors was studied at a constant sample temperature (25°C) as a function of partial pressure of ethyl acetate vapour.

It is assumed that 'm' depends on the partial pressure (p) of the reagent liquid and in the initial period, also on the time of exposure. After some time, however, an equilibrium is established. Thus we assume[25] that in the initial region

$$m(t) = Q(t) \cdot p \qquad (3.3)$$

where Q(t) is a function of time.

At equilibrium,

$$m_0 = Q_0 \cdot p \qquad (3.4)$$

where Q_0 now becomes independent of time. This is expected from Langmuir's[26] adsorption isotherm, when a small fraction of the surface is covered by the gas or vapour molecules. Combining (3.2) and (3.3), we get

$$\sigma_A \{m(t)\} = \sigma_V \exp\{\alpha \cdot Q(t) \cdot p\} \qquad (3.5)$$

and at equilibrium for (3.4),

$$\sigma_A(m_0) = \sigma_V \exp(\alpha \cdot Q_0 \cdot p) \qquad (3.6)$$

A plot of log $\sigma_A(m_0)$ or logarithm of saturation current vs. the

vapour pressure (ϕ) at equilibrium is expected from (3.6) to be linear.

In Figs. 3.11 and 3.12 we show such plots of logarithm of the saturation current versus vapour pressure (ϕ) at equilibrium for ethyl acetate adsorption on the various polyene semiconductors. Fairly good straight lines are obtained (Figs. 3.11 and 3.12). The slope of these curves (αQ_o) is a measure of the strength of interaction between the vapour molecules and the semiconductors. These linear plots prove the applicability of the Langmuir adsorption isotherm for small fraction of surface coverage in these cases of vapour adsorption on polyene crystallites.

3.3.3 Adsorption kinetics

We have examined if the adsorption kinetics follow the Roginsky-Zeldovich equation.

Integrating equation (3.1), we get,

$$m(t) = \frac{kT}{\beta} \log(t+t_o) + \text{Constant} \qquad (3.7)$$

From equations (3.2) and (3.7),

$$\log \sigma_A = \frac{\alpha kT}{\beta} \log(t+t_o) + \text{Constant} \qquad (3.8)$$

Thus, from any empirically chosen t_o, a linear plot of either log σ_A vs. log ($t+t_o$) or logarithm of current vs. logarithm of time is suggested from equation (3.8). Results in Figs. 3.13 - 3.17 for vitamin A alcohol, vitamin A acetate, β -apo-8'-carotenal, ostacene

FIG. 3.11 : Change in the dark current of vitamin A (alcohol and acetate) powder cells at 25°C as a function of the vapour pressure of ethyl acetate.
The lines (1) and (2) correspond to vitamin A alcohol (left scale) and vitamin A acetate (right scale) respectively.

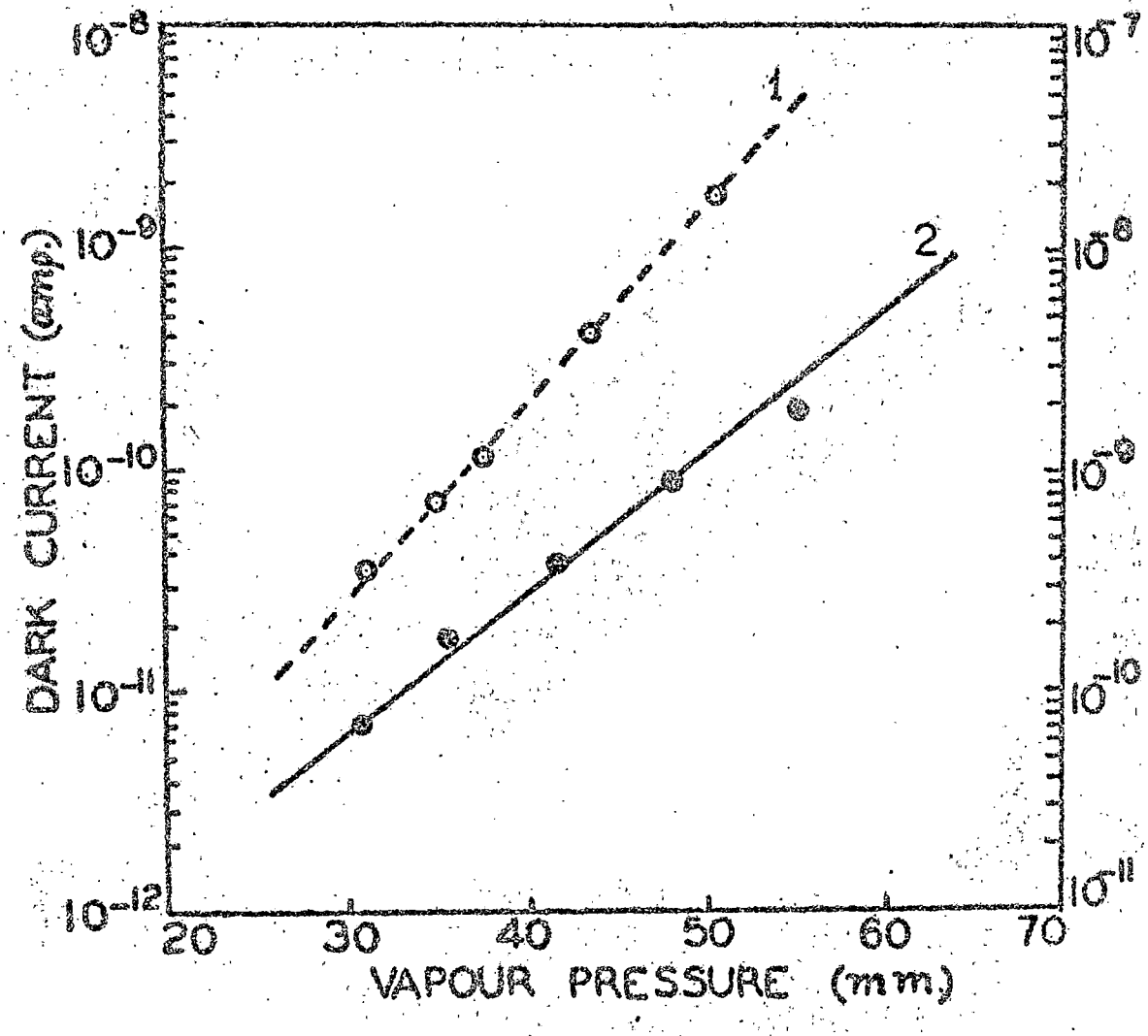
DARK CURRENT (amp.)
10⁻⁸
10⁻⁹
10⁻¹⁰
10⁻¹¹
10⁻¹²
10⁻⁷
10⁻⁸
10⁻⁹
10⁻¹⁰
10⁻¹¹
1
2
20
30
40
50
60
70
VAPOUR PRESSURE (mm.)

FIG. 3·11

FIG.3.12 : Change in the dark current of β -apo-8'-carotenal, astacene and methyl bixin powder cells kept at 25°C as a function of the vapour pressure of ethyl acetate. The lines 1, 2 and 3 correspond to β -apo-8'-carotenal, astacene and methyl bixin respectively.

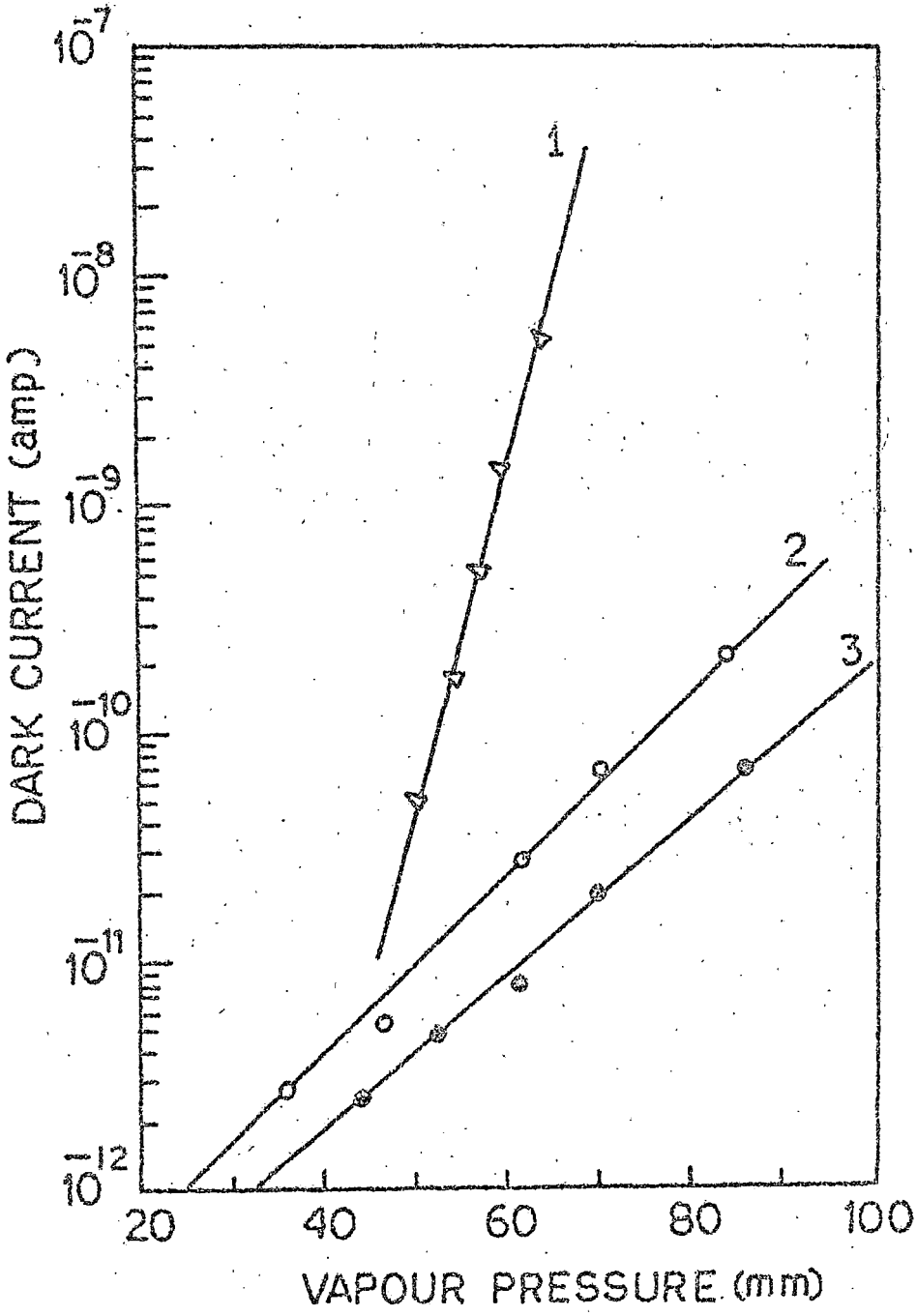
DARK CURRENT (amp.)
10^{-7}
10^{-8}
10^{-9}
10^{-10}
10^{-11}
10^{-12}
1
2
3
20
40
60
80
100
VAPOUR PRESSURE (mm)

FIG. 3·12

FIG.3.13 : Adsorption kinetics data plotted according to Roginsky-Zeldovich equation for vitamin A alcohol.

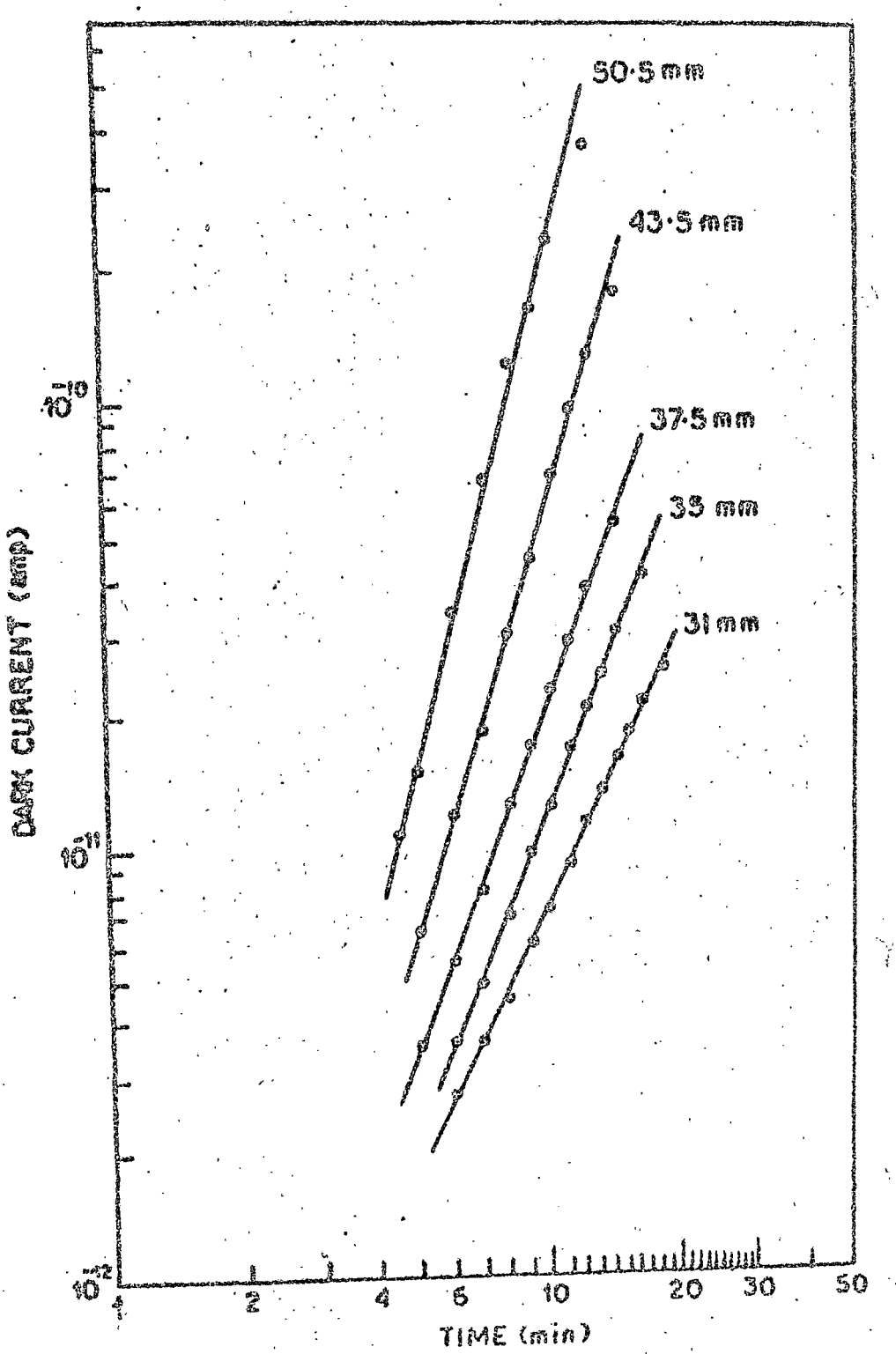
50·5 mm
43·5 mm
37·5 mm
33 mm
31 mm
DARK CURRENT (amp)
10^{-10}
10^{-11}
10^{-12}
1
2
4
6
10
20
30
50
TIME (min)

FIG. 3·13

FIG.3.14 : Adsorption kinetics data plotted according to Roginsky-Zeldovich equation for vitamin A acetate.

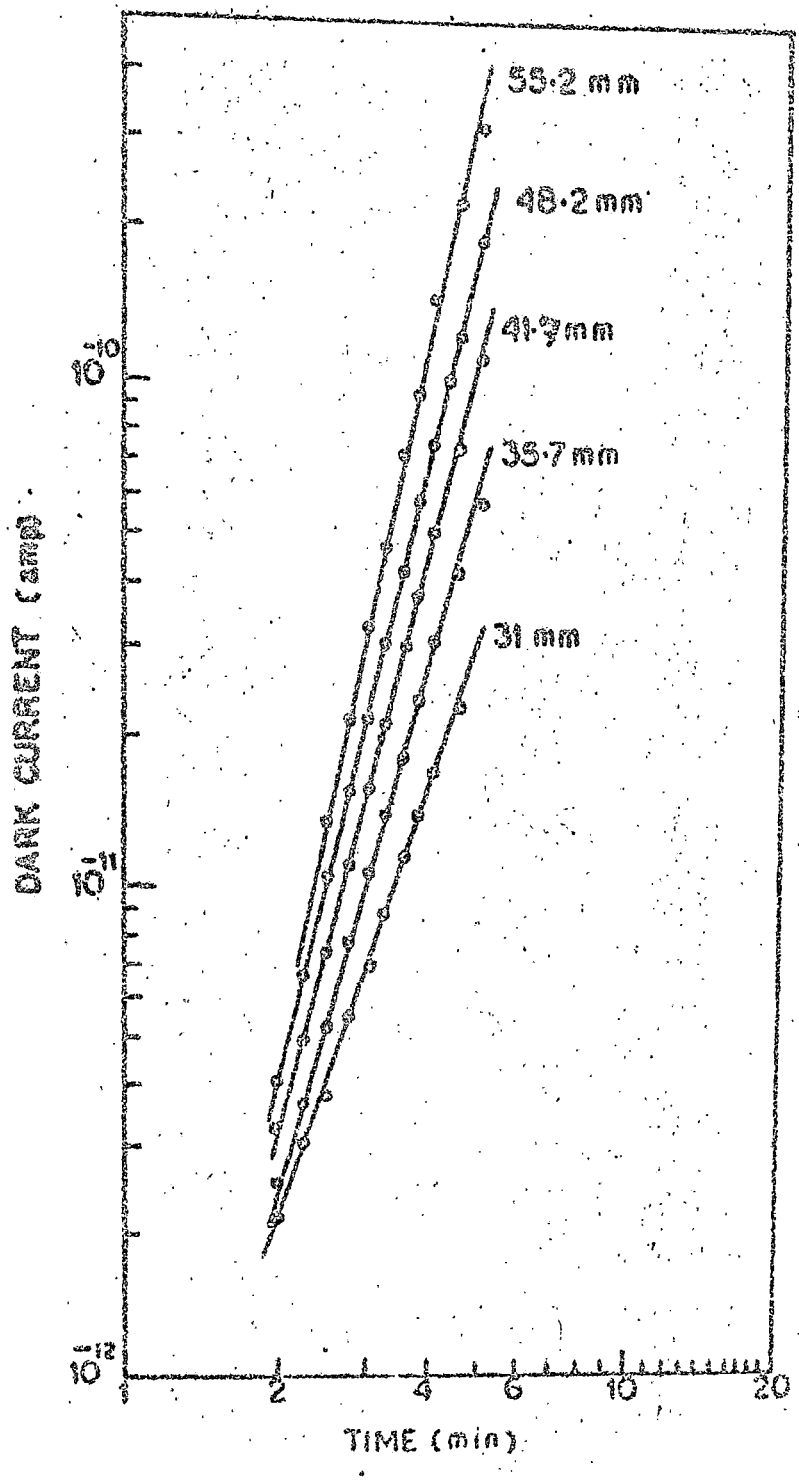
55·2 mm
48·2 mm
41·7 mm
35·7 mm
31 mm
DARK CURRENT (amp)
10^{-10}
10^{-11}
10^{-12}
2
4
6
10
20
TIME (min)

FIG. 3·14

FIG.3.15 : Adsorption kinetics data plotted according to Roginsky-Zeldovich equation for β -apo-8'-carotenal .

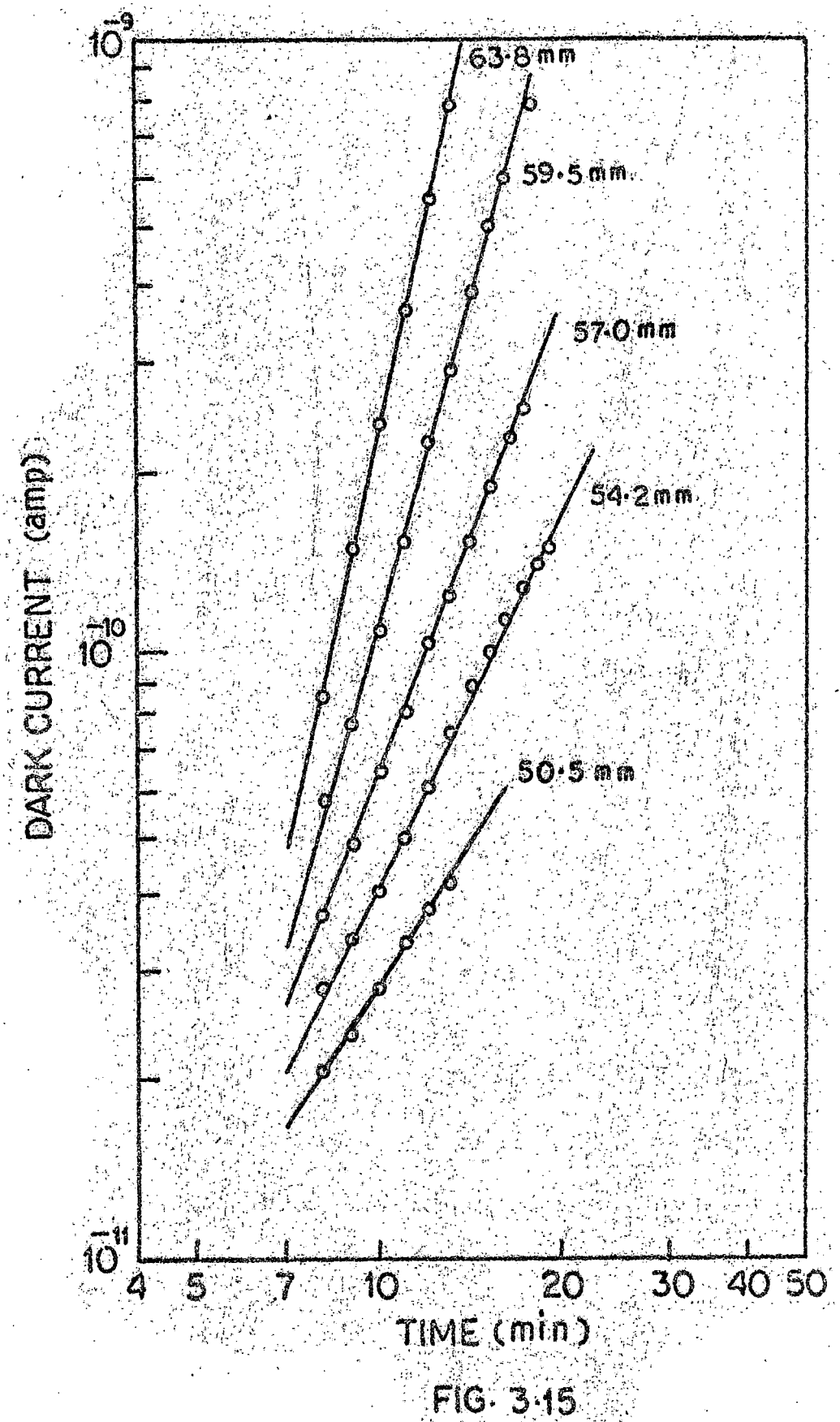
63·8 mm
59·5 mm
57·0 mm
54·2 mm
50·5 mm
DARK CURRENT (amp)
10^{-9}
10^{-10}
10^{-11}
4
5
7
10
20
30
40
50
TIME (min)

FIG. 3·15

FIG.3.16 : Adsorption kinetics data plotted according to Roginsky-Zeldovich equation for antacene.

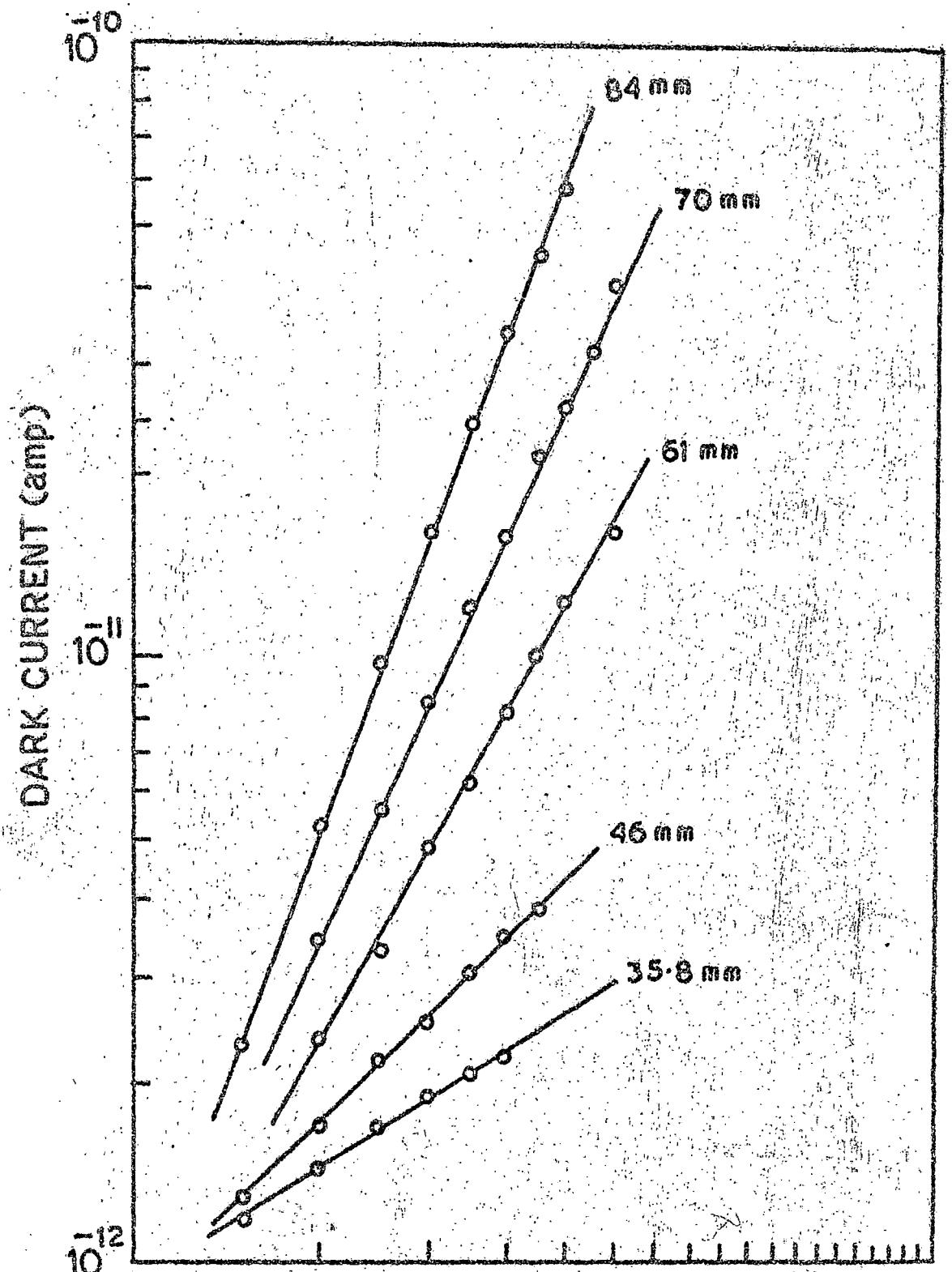
10^{-10}
10^{-11}
10^{-12}
DARK CURRENT (amp)
84 mm
70 mm
61 mm
46 mm
35·8 mm
1
2
4
6
10
20
TIME (min)

FIG. 3.16

FIG.3.17 : Adsorption kinetics data plotted according to Roginsky-Zeldovich equation for methyl bixin.

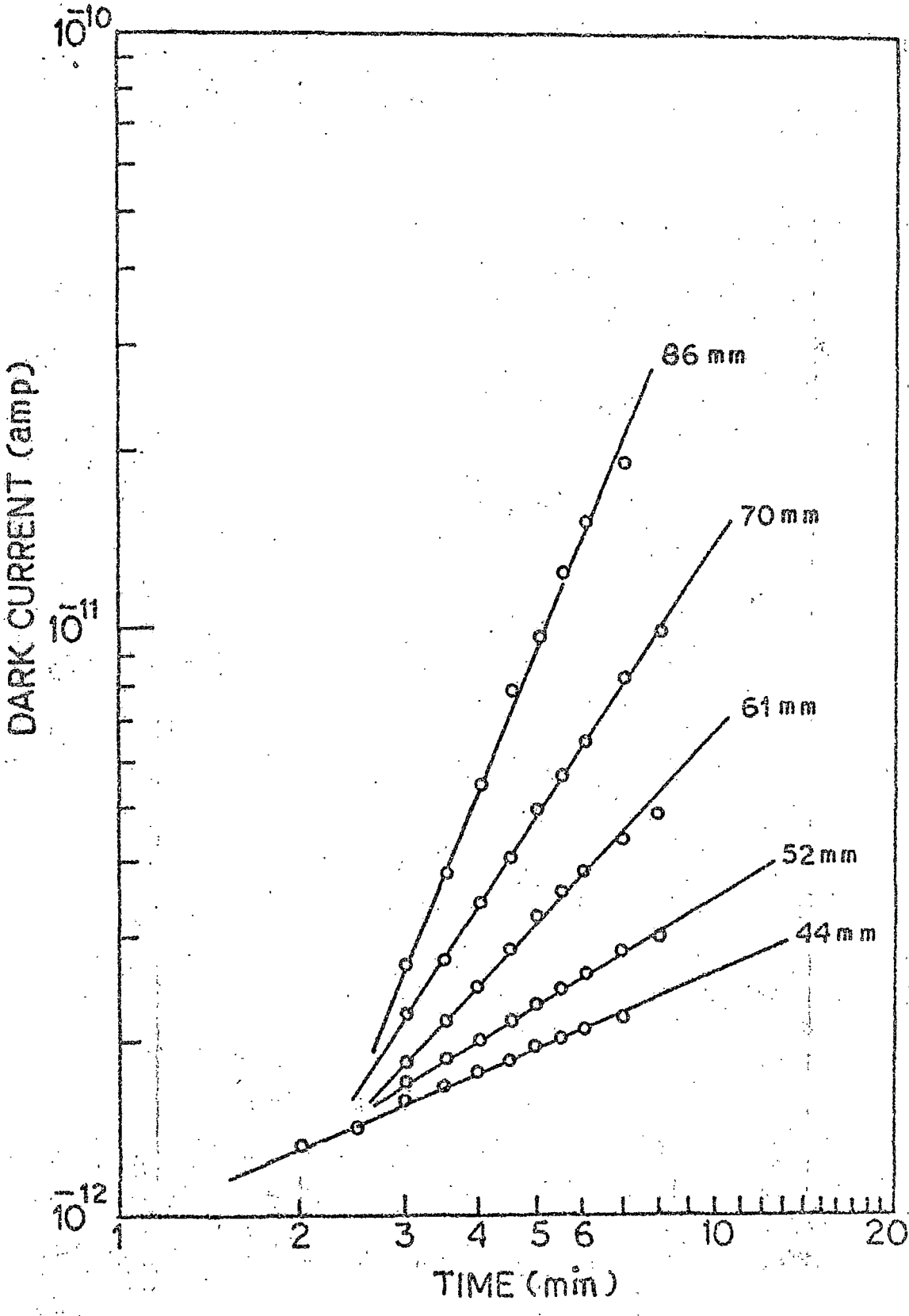
10^{-10}
10^{-11}
10^{-12}
DARK CURRENT (amp)
86 mm
70 mm
61 mm
52 mm
44 mm
1
2
3
4
5
6
10
20
TIME (min)

FIG. 3.17

and methyl bixin respectively are in good agreement with this. In the initial region, different slopes observed at different vapour pressures show the vapour pressure-dependence of β (since α is pressure independent). The higher the partial vapour pressure, the larger is the slope. This justifies the assumption made in expression (3.3) and shows an inverse relationship between p and β. As we are unable to estimate a numerical value of α from this experiment, we can not evaluate the numerical value of β from the measured slopes. However, we have estimated the values of β/α $(=\beta')$ from the slopes to see its pressure dependence. In table 3.3 variation of β' with vapour pressure is shown.

3.3.4 Desorption Kinetics

Equation (3.1) is valid for the rate of adsorption. Since desorption is a reverse process of adsorption, expression for the rate of desorption can be written in a similar form with a positive sign in the exponent i.e., by

$$-\frac{dm}{dt} = A^* \exp\left(\frac{\beta^* m}{RT}\right) \qquad (3.9)$$

Here $\beta^* m$ is the activation energy for desorption. In the measurement of desorption, the experimental condition is so arranged that there is no re-adsorption. The plots of logarithm of current vs. logarithm of time for desorption of ethyl acetate vapour from vitamin A alcohol, vitamin A acetate, β -apo-8'-carotenal, octacene and methyl bixin crystallites are shown in Figs. 3.18 - 3.22 respectively.

Table - 3.3

Vapour pressure dependence of the factor β' for ethyl acetate vapour adsorption kinetics.

Polyenes	Vapour pressure (mm)	β' (eV)
Vitamin A alcohol	31.0	1.202×10^{-2}
	35.0	1.005×10^{-2}
	37.5	0.930×10^{-2}
	43.5	0.759×10^{-2}
	50.5	0.648×10^{-2}
Vitamin A acetate	31.0	0.819×10^{-2}
	35.7	0.758×10^{-2}
	41.7	0.660×10^{-2}
	48.2	0.601×10^{-2}
	55.2	0.518×10^{-2}

contd.

Table - 3.3 (contd.)

Polyenes	Vapour pressure (mm)	β' (eV)
	50.5	1.629×10^{-2}
β -apo-8'-	54.2	1.245×10^{-2}
Carotenal	57.0	0.994×10^{-2}
	59.5	0.718×10^{-2}
	63.8	0.555×10^{-2}
	35.8	3.973×10^{-2}
Astacene	46.0	2.568×10^{-2}
	61.0	1.422×10^{-2}
	70.0	1.168×10^{-2}
	84.0	0.931×10^{-2}
	44.0	5.714×10^{-2}
Methyl	52.0	4.131×10^{-2}
bixin	61.0	2.526×10^{-2}
	70.0	1.638×10^{-2}
	86.0	1.039×10^{-2}

FIG. 3.18 : Desorption kinetics data plotted according to Roginsky - Zeldovich equation for vitamin A alcohol.

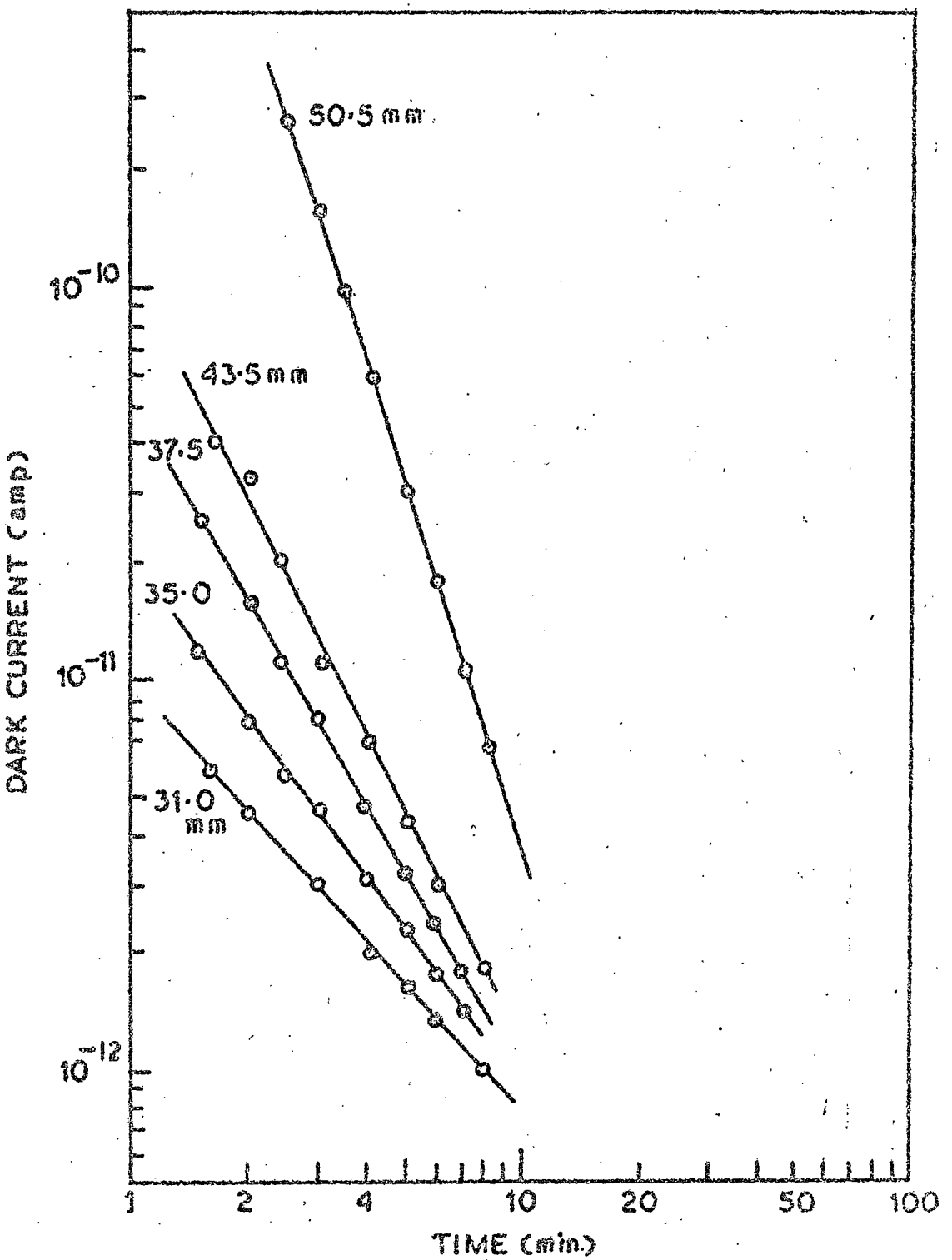
50·5 mm
43·5 mm
37·5
35·0
31·0 mm
10^{-10}
10^{-11}
10^{-12}
DARK CURRENT (amp.)
1
2
4
10
20
50
100
TIME (min.)

FIG. 3·18

Fig.2.13 : Desorption kinetics data plotted according to Roginsky-Zeldovich equation for vitamin A acetate.

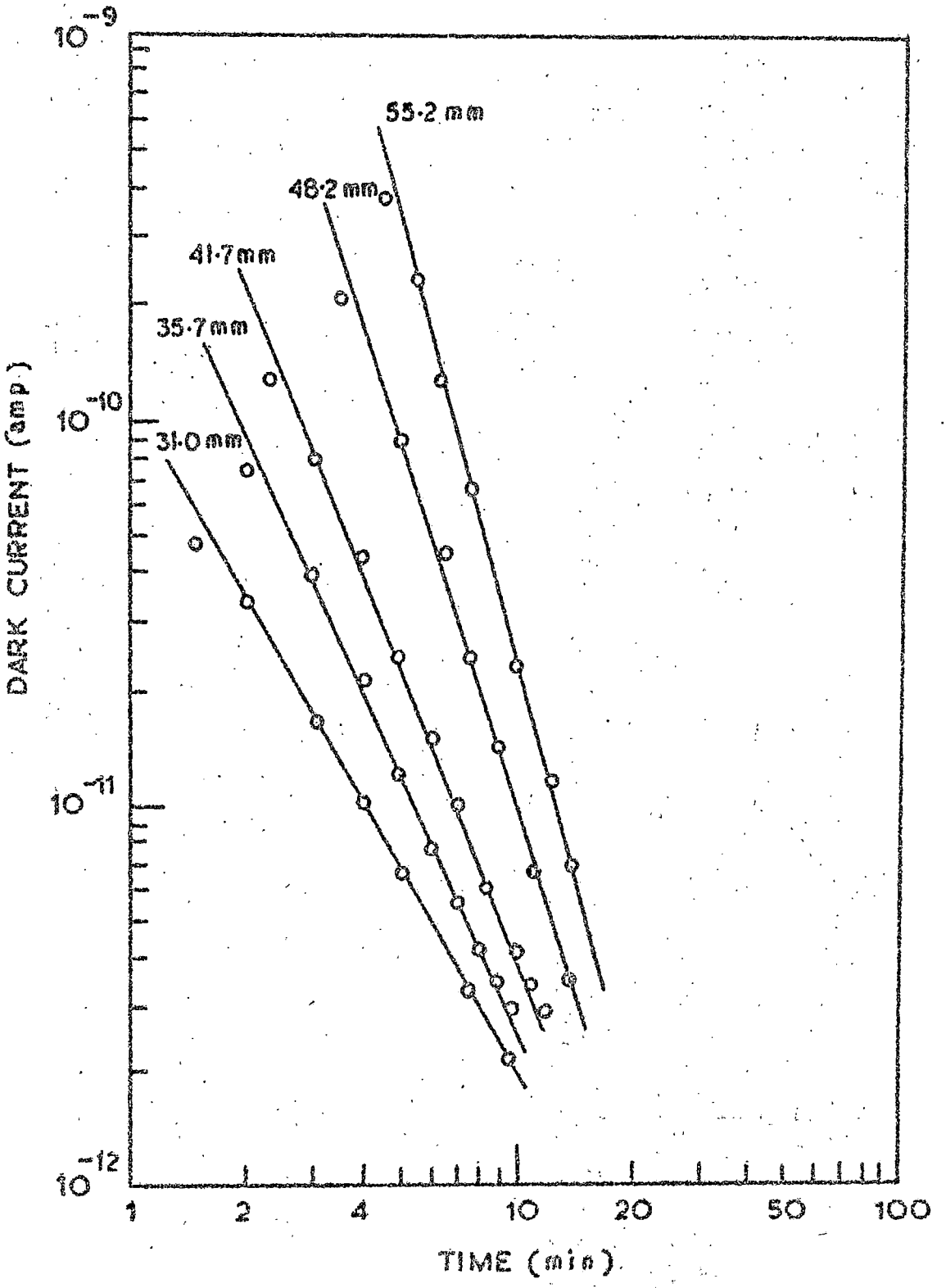
DARK CURRENT (amp)
10^{-9}
10^{-10}
10^{-11}
10^{-12}
55·2 mm
48·2 mm
41·7 mm
35·7 mm
31·0 mm
1
2
4
10
20
50
100
TIME (min)

FIG. 3·19

FIG. 3.20 : Desorption kinetics data plotted according to Roginsky-Zeldovich equation for β -apo-8'-carotenal.

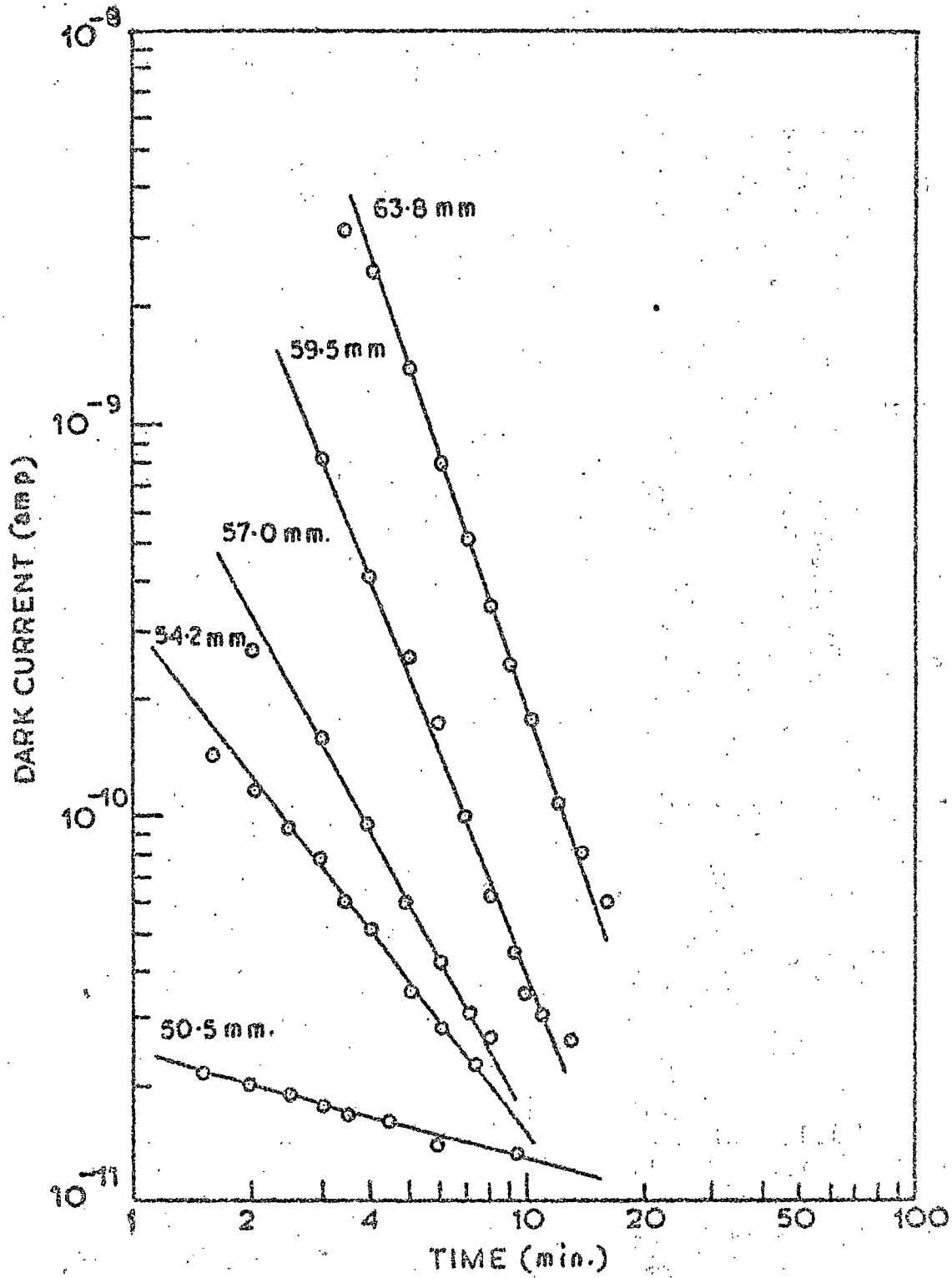
DARK CURRENT (amp)
10^{-8}
10^{-9}
10^{-10}
10^{-11}
63·8 mm
59·5 mm
57·0 mm.
54·2 mm
50·5 mm.
1
2
4
10
20
50
100
TIME (min.)

FIG. 3·20

FIG.3.21 : Desorption kinetics data plotted according to Roginsky - Zeldovich equation for ostacene.

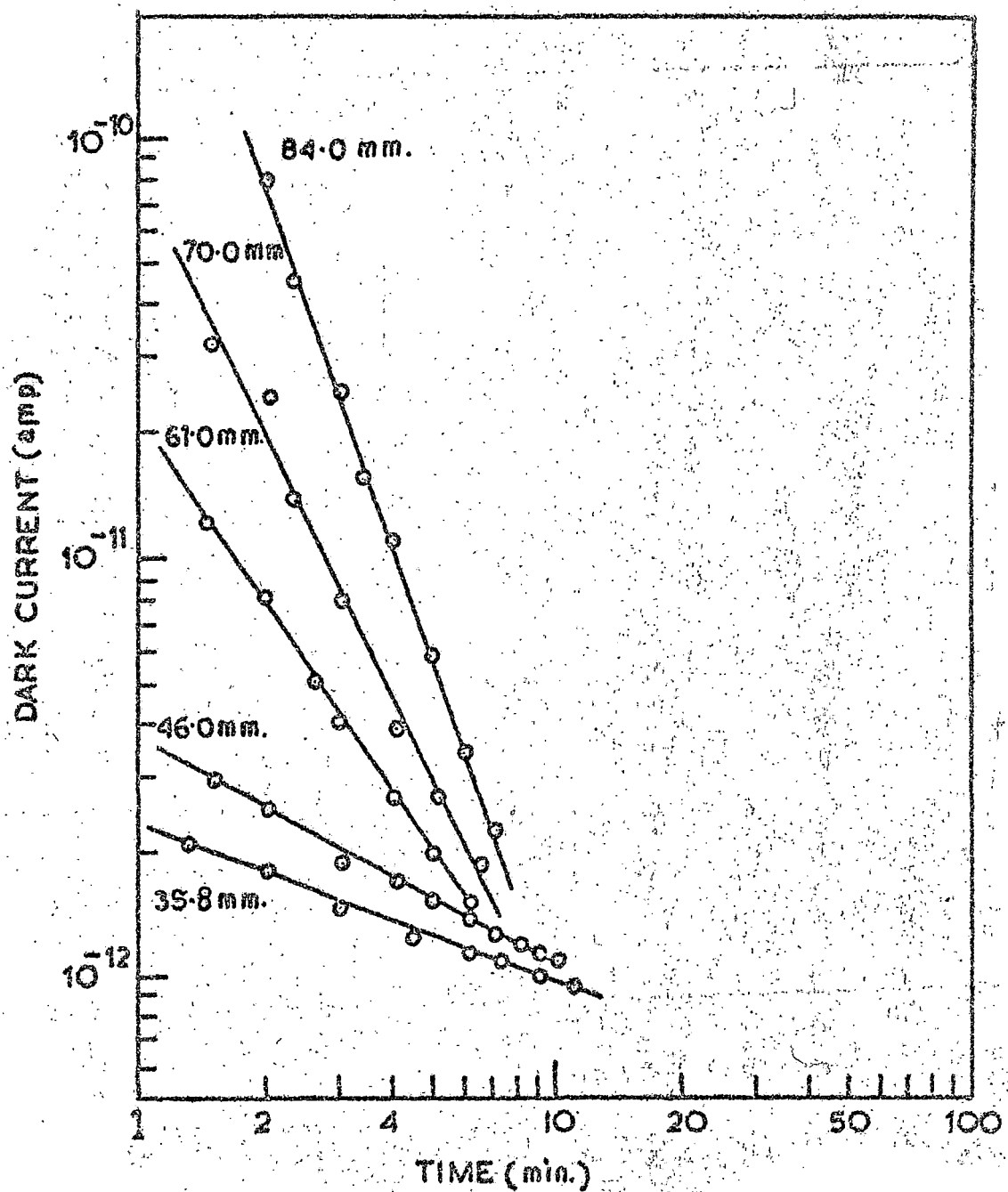
84·0 mm.
70·0 mm.
61·0 mm.
46·0 mm.
35·8 mm.
10^{-10}
10^{-11}
10^{-12}
DARK CURRENT (amp)
1
2
4
10
20
50
100
TIME (min.)

FIG. 3·21

FIG.3.22 : Desorption kinetics data plotted according to Roginsky-Zeldovich equation for methyl bixin.

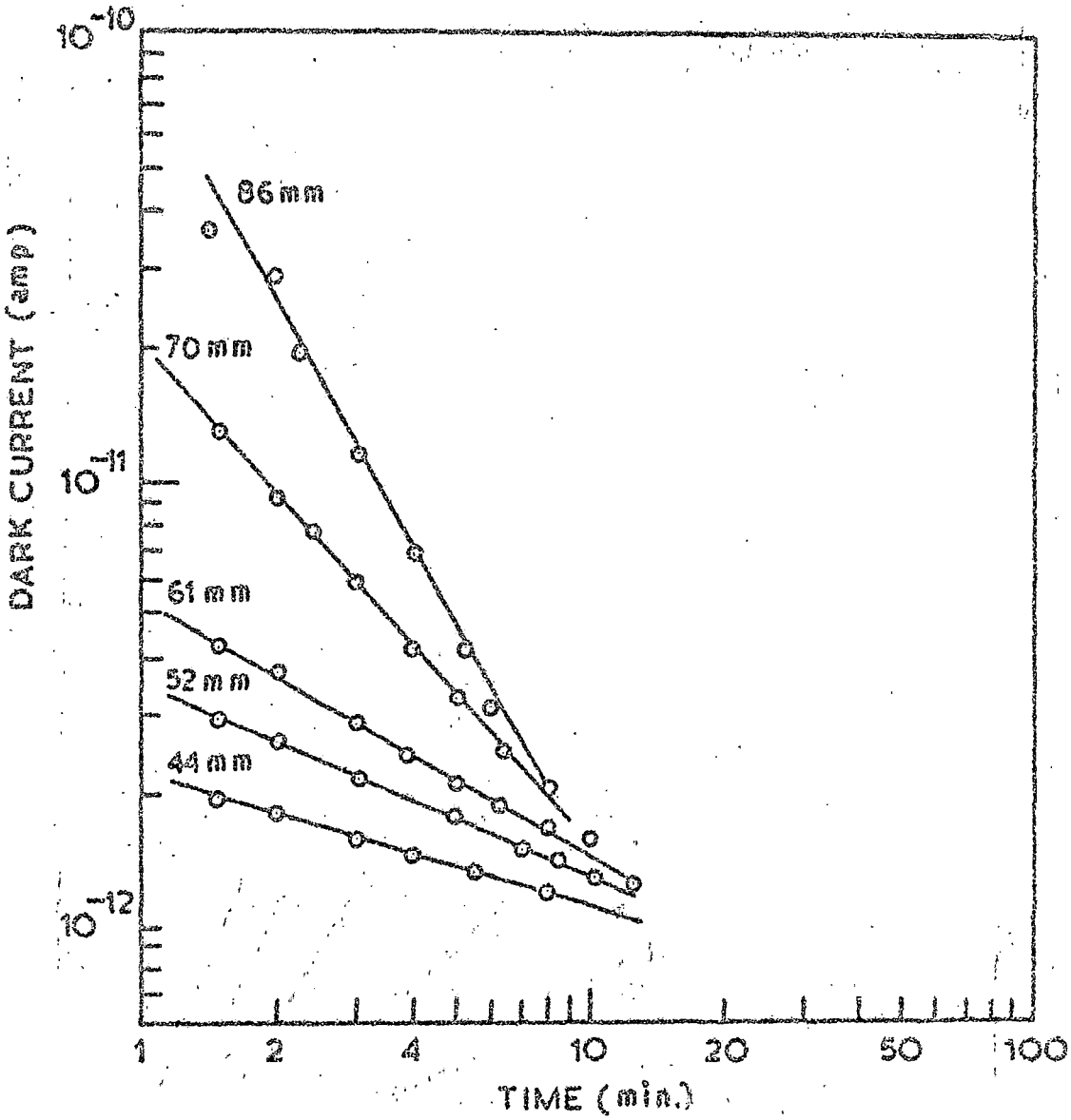
DARK CURRENT (amp)
10^{-10}
10^{-11}
10^{-12}
86 mm
70 mm
61 mm
52 mm
44 mm
1
2
4
10
20
50
100
TIME (min.)

FIG. 3·22

In table 3.4, we present the experimental values of $\beta^{*\prime}$ $(= \beta^*/\alpha)$ obtained from these plots for ethyl acetate vapour desorption from different polyene crystallites. As like that β, β^* also decreases with increasing vapour pressure. For any particular pressure of ambient vapour, β^* is larger than β.

There are number of different treatments[27] for the Roginsky-Zeldovich equation. A simple two stage-process after Riley and Leslie[16] as shown in Fig. 3.23 seems quite satisfactory to account for the experimental observations. In the first stage, a mobile van der Waals adsorption on the crystal surface gives a Lennard-Jones potential energy curve which is assumed to depend on the fraction of surface coverage. This stage is followed by a rate-determining transition over a potential energy barrier to the final stage of adsorption forming weakly bound complexes between the vapour molecules and the polyene crystallites. The barrier is formed by the intersection of the two potential curves. As more vapour molecules get physically adsorbed (van der Waals), a repulsive interaction between the dipoles will raise the potential energy curve for the first stage thereby lowering the barrier height giving decreasing activation energy of adsorption with increasing vapour pressure. As the surface coverage of the second stage rises, this potential curve also rises resulting in lowering of desorption activation energy with increasing pressure. The rise of the second stage curve is such that the minimum of this curve is always at lower energy than the minimum of the first stage, the energy difference between these two minima decreasing with increasing vapour pressure.

Table - 3.4

Vapour pressure dependence of the factor $\beta^{*\prime}$ for ethyl acetate vapour desorption kinetics.

Polyenes	Vapour pressure(mm)	$\beta^{*\prime}$ (eV)
Vitamin A alcohol	31.0	2.304×10^{-2}
	35.0	1.847×10^{-2}
	37.5	1.492×10^{-2}
	43.5	1.201×10^{-2}
	50.5	0.798×10^{-2}
Vitamin A acetate	31.0	1.431×10^{-2}
	35.7	1.151×10^{-2}
	41.7	1.023×10^{-2}
	48.2	0.802×10^{-2}
	55.2	0.648×10^{-2}

contd.

Table - 3.4 (contd.)

Polyenes	Vapour pressure (mm)	$\beta^{x'}$ (eV)
β -apo-8'-carotenal	60.5	8.621×10^{-2}
	64.2	1.919×10^{-2}
	57.0	1.322×10^{-2}
	50.5	1.015×10^{-2}
	63.8	0.808×10^{-2}
Astacene	35.8	6.733×10^{-2}
	46.0	4.591×10^{-2}
	61.0	1.720×10^{-2}
	70.0	1.250×10^{-2}
	84.0	0.969×10^{-2}
Methyl bixin	44.0	8.312×10^{-2}
	52.0	5.971×10^{-2}
	61.0	4.322×10^{-2}
	70.0	2.215×10^{-2}
	86.0	1.421×10^{-2}

FIG. 3.23 : Potential energy curves for vapour adsorption in two stages in polyenes, explaining modified Roginsky-Zeldovich plots. E_d^1, E_d^2 and E_d^3 are activation energies of desorption in order of increasing pressure. Similarly E_a's are activation energies for adsorption.

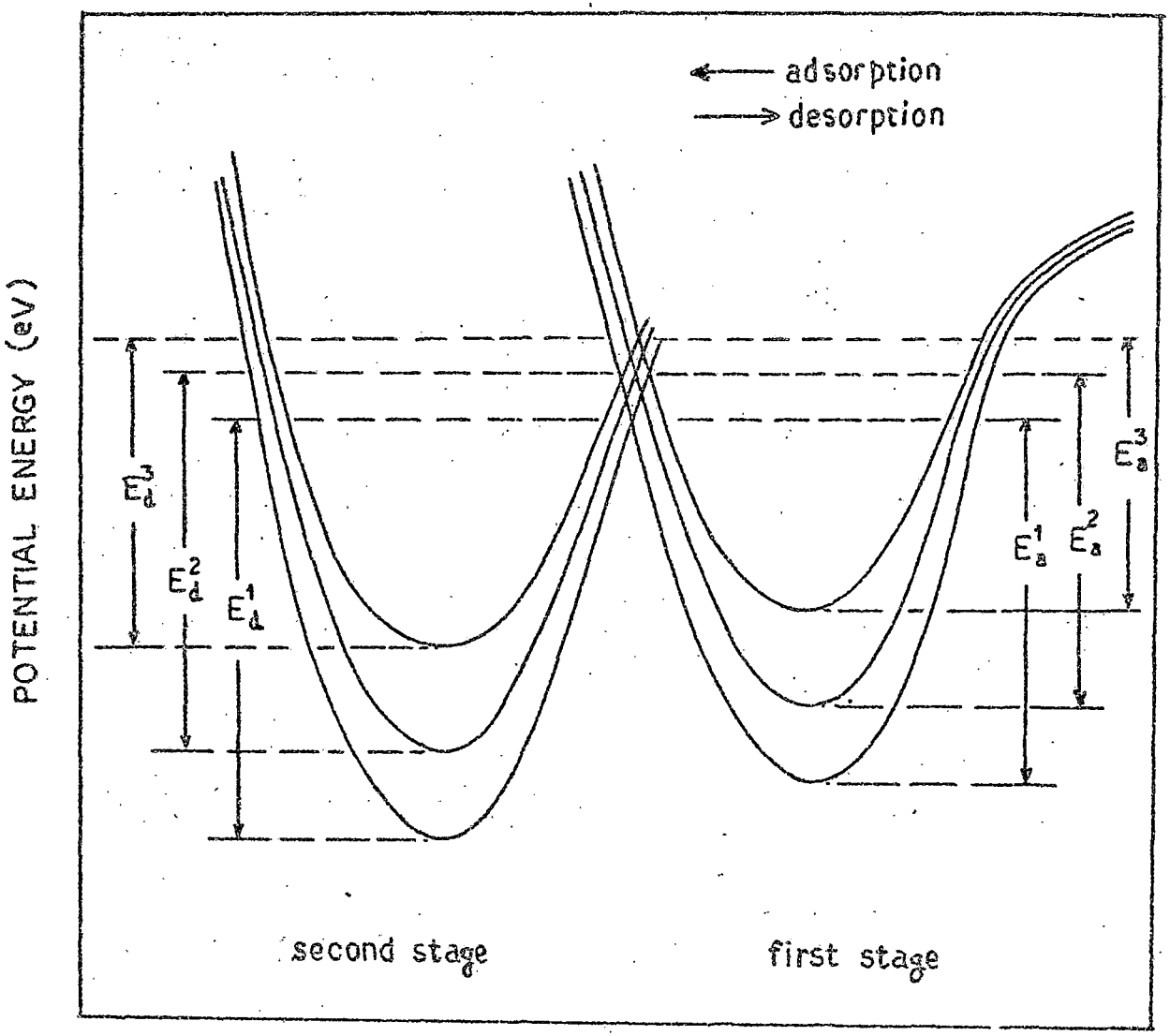
adsorption
desorption
POTENTIAL ENERGY (eV)
E_d^3
E_d^2
E_d^1
E_a^1
E_a^2
E_a^3
second stage
first stage
REACTION PATH

FIG. 3·23

Here β^*_m, the activation energy for desorption should, apart from a small entropy factor, be equal to the vapour-surface molecular complex. In table 3.4, we have shown the experimental values of $\beta^{*\prime}$. Unfortunately neither our experiments give any numerical value of α, nor we have been able to measure n, the amount of vapour adsorbed. Any reliable estimate of the binding energy of various vapours with different polyenes has therefore, not been possible. In case of hydration of proteins, Rosenberg[18] estimated $\alpha \approx 2.6$. A similar value of α for these cases of vapour desorption from polyene crystallites, the value of binding energy are $\approx 10^{-2}$ eV per unit of 'm' desorbed. This low value of the binding energy accounts for easy and efficient desorption of these vapours from the polyene crystals.

3.4 Conclusion

The adsorption of vapours enhances the semiconductivity of the polyenes appreciably. This enhancement depends on the chemical nature and also on the pressure of the adsorbed vapour. The adsorption and desorption kinetics follow the modified Roginsky-Zeldovich relation. A two stage adsorption process, the first stage of which gives a Lennard - Jones potential energy curve and is followed by a rate-determining transition over a potential energy barrier to the second state of adsorption forming weakly bound complexes between the vapour molecules and the polyene crystallites, can explain satisfactorily the experimentally observed kinetics data.

References

1) A.T. Vartanyan, Zhur. Fiz. Khim., 22, 769 (1948).

2) A.T. Vartanyan, Doklady Akad. Nauk. S.S.S.R., 71, 641 (1950).

3) A.G. Chynoweth, J. Chem. Phys., 22, 1029 (1954).

4) B. Rosenberg, J. Chem. Phys., 34, 812 (1961).

5) K.M. Jain, A. Ghosh, B. Mallik and T.N. Misra, Indian J. Phys., 52A, 643 (1978).

6) T.N. Misra, B. Rosenberg and R. Switzer, J. Chem. Phys., 48, 2096 (1968).

7) O. Fritsch, Ann. Physik, 22, 375 (1935).

8) W. Hartmann, Z. Physik, 102, 709 (1936).

9) W. Mayer and H. Neldel, Physik, Z.38, 1014 (1937).

10) T.J. Gray and P.W. Darby, J. Chem. Phys., 60, 201 (1956).

11) A. Bree and L.E. Lyons, J. Chem. Soc., 5 179 (1960).

12) A. Bree and L.E. Lyons, 25, 384 (1956).

13) B. Rosenberg and J.F. Camiscoli, J. Chem. Phys., 35, 932 (1961).

14) W.G. Schneider and T.C. Waddington, J. Chem. Phys., 25, 358 (1956).

15) D. D. Eley and R.B. Leslie, Advances in Chemical Physics (New York: Interscience Publishers) 7, 238 (1964).

16) Ya. Zeldovich, Acta Physicochim URSS, 1, 449 (1934).

17) S. Roginsky and Ya. Zeldovich, Acta Physicochim URSS, 1, 554, 595 (1934).

18) B. Rosenberg, Physical Processes in Radiation Biology edited by L. Augenstein, R. Mason and B. Rosenberg (Academic Press, New York and London, 1964) p 111.

19) S. Treiber and M. Koren, Natt. Bur. Stand. Circ., 514 (1951).

20) F. Gutmann and L.E. Lyons, Organic Semiconductors (John Wiley and Sons, New York, London and Sydney, 1967) p 669.

21) J.C. Lorquet, Mol. Phys., 9, 101 (1965).

22) M.M. Labes and O.N. Rudyj, J. Am. Chem. Soc., 85, 1955(1963).

23) P.J. Neucroft, O.N. Rudyj and M.M. Labes, J. Am. Chem. Soc., 85, 2059 (1963).

24) P.J. Neucroft, O.N. Rudyj, R.F. Salomon and M.M. Labes, J. Phys. Chem., 66, 779 (1962).

25) B. Mallik, A. Ghosh and T.N. Misra, Proc. Indian Acad. Sci., 93A, 25 (1979).

26) S. Glasstone, Text Book of Physical Chemistry (Macmillan and Co. Ltd., London, 1951) p 1200.

27) F.S. Stone, Chemistry of the solid state edited by W.E. Garner (Butterworths, London, 1955) p 367.